SPECIFIC AIMS:

Bacterial cell-surface glycans influence host recognition and are considered key virulence determinants. The endogenous oral pathogen *Porphyromonas gingivalis* (*Pg*) displays at least three different types of cell surface glycans; two types of lipopolysaccharides (O-LPS and A-LPS), and K-antigen capsule. Research has demonstrated the importance of these surface glycans in *Pg* pathogenesis through several mechanisms: including immune evasion, immune modulation, and biofilm development. Yet, the precise genes involved in synthesis of these surface glycans and how synthesis is regulated remains to be determined. This gap in knowledge limits our understanding of Pg's pathogenic potential.

The long-term goal of our research program is to elucidate the regulatory mechanisms and environmental and nutritional parameters that control the expression of genes involved in modifying the surface properties of *Pg*, and to determine how changes in synthesis relate to biofilm persistence and pathogenicity. Our overarching model is that the biofilm state acts as a reservoir of bacterial cells while K-antigen capsule synthesis marks the transition to virulence and disruption of homeostasis. Towards our goal, we have shown that two DNABII family members in *Pg* (HU PG0121 and HU PG1258) are involved in controlling production of capsule. In general, DNABII proteins are known to be critical for regulation of cell metabolism, the response to environmental perturbations, and in controlling the transition to and from a quiescent state. Central to our studies is an antisense RNA (asSuGR, for antisense Surface Glycan Regulator) encoded at the 5'-end of the capsule locus (PG0104-PG0121) within a novel 77bp inverted repeat (77bpIR) element. Deletion or over-expression of asSuGR alters the synthesis of LPS and K-antigen capsule and expression is, in part, controlled by a two-component response regulator PG0720. In addition, we have determined that synthesis of sphingolipids (SLs) influences the presentation of K-antigen capsule on the cell surface, and this finding aligns with our discovery of a matching asSuGR target sequence in an SL-synthesis locus (PG1780 – PG1788), suggesting that capsule and SL-synthesis are coordinated by asSuGR.

The central hypothesis of this project is that asSuGR is a cis and trans-acting molecule that controls changes in cell surface properties by coordinating expression levels of genes involved in synthesis of surface glycans and SLs and thus plays a fundamental role in modulating *Pg* virulence. To test this hypothesis, we will use our collection of Pg glycan mutants, genomics, and biochemical techniques to determine how expression of asSuGR is controlled and how the 77bpIR element is involved in regulating the synthesis and presentation of capsule and LPS. We will also elucidate the activation signal(s) or metabolite(s) for the PG0719-PG0720 two-component system which will allow us to better understand its exact role in controlling the Pg's surface properties in response to altering oral environments. To this end, we will pursue the following Aims:

AIM 1. How does the 77bpIR region encoding asSuGR control expression of surface glycans? The goal of this aim is to use genetics and a variety of biochemical techniques to determine how expression of the antisense RNA molecule asSuGR is controlled and how the 77bpIR element influences the cell surface presentation of K-antigen capsule and LPS.

AIM 2. Characterization of *P. gingivalis* DNABII proteins (PG0121 and PG1258). The goal of this Aim is to use a variety of biochemical techniques, including EMSA and surface plasmon resonance, as well as ChIP-Seq analysis to determine how HU PG0121 and HU PG1258 control expression levels of the K-antigen operon and to identify regions of the chromosome where these DNABII proteins interact.

AIM 3. Heme sensing by the two-component sensor PG0719. The goal of this Aim is to identify and characterize the activation signal or metabolites sensed by the two-component sensor PG0719 at the atomic level. We will also probe and decipher the conformational changes associated with signal transduction within this signaling pathway to obtain mechanistic insights. Published and preliminary data strongly support the premise that PG0719 is a heme sensor.

Impact of the proposed research. Little is known about the molecular mechanisms or the environmental parameters that regulate synthesis of Pg surface glycans or if expression of genes involved in K-antigen synthesis and the synthesis of other cell surface structures is coordinated. This gap in knowledge limits our understanding of *Pg* as a pathogen. Until the mechanisms that control capsule expression are determined, methods toward hypothesis driven therapeutics against the virulence and dissemination of *Pg* and its subsequent role in periodontal and other systemic diseases are limited.

RESEARCH STRATEGY
(A) SIGNIFICANCE

Porphyromonas gingivalis (*Pg*) is an endogenous oral pathogen, strongly implicated in the etiology of periodontal disease; a chronic inflammatory pathology that leads to the destruction of tissues supporting the teeth (1-4) and synthesis of a capsule is a key virulence determinant (5). Encapsulation is a well-known mechanism that protects pathogenic bacteria from clearance by host immune defenses (6). This reduction in clearance can lead to persistent survival and thereby long-term interplay between the bacterium and host. Capsules not only reduce the ability of the host effectors to gain access to the bacterial cell, but also mask the cell surface and modulate the host's response to the bacterium. This model is supported by studies showing that bacteria that cloak themselves in a capsule have an advantage in immune evasion (7). Strains of *Pg* that produce a capsule are more resistant to phagocytosis (8), and cause a spreading type of infection in a murine lesion model (9). In contrast, non-encapsulated *Pg* strains adhere more readily to cultured primary gingival epithelial cells and cause a localized abscess (10). In addition, a capsule null mutant strain was shown to be a more potent inducer of cytokine synthesis by human gingival fibroblasts, indicating a role for capsule in cloaking *Pg* against innate immune responses (5). Recent studies showed that infections with strains that produce K-antigen (K1 and K2 serotypes) can induce neuroinflammation, astrogliosis, cognitive decline, and histopathological signs of Alzheimer's disease in the hippocampus of rats (11), which aligns with earlier studies showing that purified capsule (again, in particular K-1 and K-2 serotypes) elicit chemokine production from phagocytic cells, suggesting that the host response to this antigen may contribute to the formation of the inflammatory cell lesion observed during Pg-elicited periodontal disease. Although it is becoming evident that synthesis of K-antigen capsule is an important virulence determinant (11), its involvement and the role of other surface glycans (A-LPS and O-LPS) in the overall deregulation of host responses is not fully understood.

Loci and regulatory mechanisms known to control synthesis of *Pg* surface glycans. Sequence analysis of the *Pg* genome indicates multiple glycan synthesis loci (12), but which genes synthesize the different surface glycans (K-antigen capsule, O-LPS, and A-LPS) is not clear. Genes in the PG0104-PG0121 locus (strain W83) are required for K1-capsule synthesis (13, 14). Yet, a PG0106 mutant strain is also deficient in lipopolysaccharide (LPS) synthesis (15). These findings indicate that PG0106 and possibly other genes in the K-antigen locus are involved in synthesizing both K-antigen capsule and LPS. The K-antigen locus encodes a large polycistronic transcript of ~19.4 kb, as well as multiple monocistronic and additional polycistronic messages (16, 17). The coding sequence of another polysaccharide synthesis locus (PG1135-PG1142) is also highly conserved in various *Pg* strains (13), and the genes in this locus have been shown to be involved in anionic polysaccharide (APS) biosynthesis (18, 19). A tyrosine phosphatase (Ltp1) encoded by PG1641 that controls expression of a variety of surface polysaccharide synthesis genes has also been identified (20-22) and we have determined that HU PG0121 (see below) also controls production of surface polysaccharides (16, 17), specifically genes in both the K-antigen locus and the APS locus. In addition, we have shown that the response regulator PG0720 activates expression of a highly conserved antisense RNA (designated asSuGR for antisense surface glycan regulation) that originates from within a 77bp inverted repeat element located at the 5' end of the capsule locus, and whose expression results in higher transcript levels of genes in the capsule operon (23). The sequence and positioning of asSuGR and its predicted function are shown in preliminary studies (Fig 1). The impact of asSuGR and the 77bpIR element on gene regulation and Pg's pathogenic potential is a primary focus of this research program.

DNABII family of protein function. *Pg* has two members of the DNABII (DNA binding and bending) proteins, PG0121 (discussed above) and PG1258. DNABII proteins are a homologous family of proteins of highly similar primary and secondary structure that are comprised of two forms, HU and IHF. HU was originally discovered in a ribosomal fraction from *E. coli* (24), and subsequent purification showed that it readily condensed DNA much the way histones do, thus they are commonly referred to as nucleoid-associated proteins (NAPs). HU orthologues are typically 90 to 105 amino acids, share 20 to 70% amino acid identity and are found in virtually every bacterial species. The active protomer is either homo- or hetero-dimeric depending on the bacterial species. Interestingly, an HU deficiency in *E. coli* has a mild phenotype while HU appears to be essential in *B. subtilis* and all other Gram-positive bacteria tested to date (25-27). The structure of the HU protomer is also highly conserved. Individual subunits dimerize within a conserved hydrophobic core and possess protruding antiparallel beta ribbon sheets. It is the beta ribbon from each subunit that makes the initial contact with the DNA (27). The tips at the turn of these ribbons insert/intercalate into the DNA, melting/kinking the local DNA, and resulting in enhanced DNA flexibility. Functions attributed to HU's typically involve changes in DNA architecture (27) and include gene regulation, replication initiation, and maintenance of DNA topology (HU restrains supercoils). In addition, *E. coli* IHF, a close relative of HU, also affects transcription, yet through site specific supercoiling (28). While HU protomers bind DNA in a sequence independent fashion, IHF protomers

(both homodimers as well as heterodimers) (29-33) bind to specific sequence sharing the consensus WATCAANNNNTTR (where W is A or T, N is any nucleotide and R is a purine (34)). Finally, three other key functions of HU, its ability to stimulate transcription (35), and translation (36), and its ability to bind to similar structures in DNA and RNA (37) are relevant to our studies.

Two-component systems in Pg. Two-Component Systems (TCS) are the predominant signal transduction and regulatory systems employed by bacteria to monitor, respond, and adjust to environmental changes. TCSs can directly or indirectly sense various small molecules, ions, toxins, dissolved gases, temperature, pH, osmotic pressure, light, or the cellular redox state, although, for most of them, the actual signals remain unknown (38). Although Pg experiences numerous environmental conditions in the oral cavity, surprisingly, its genome contains only four TCS pairs, along with one orphan histidine kinase, two orphan response regulators, and one chimeric TCS (12). One of these TCS pairs is the PG0719-PG0720 (also known as HaeSR) which regulates a suite of genes involved in the acquisition and uptake of iron/hemin (39). Following our recent characterization of the PG0720 response regulator and its role in up-regulating genes in the capsule operon (23) we aim to determine and characterize the precise activation signal for its conjugated sensor histidine kinase, PG0719 (Aim 3). This information, in turn, will allow us to better understand a molecular switch involved in activating the pathogenic state of Pg.

RNA-binding proteins and antisense RNA. Transcriptome studies have discovered that extensive transcription of non-coding RNAs and pervasive antisense transcription occurs in bacteria (40, 41). A number of review articles (40, 42-51) have summarized the mechanisms by which sRNAs interact with targets. Importantly, although the interaction is dynamic, all RNA is bound to proteins throughout its lifecycle. One fundamental discovery of sRNAs is these molecules form critical *in vivo* complexes with proteins, such as the carbon storage regulator protein CsrA (52); and the highly conserved RNA chaperone, Hfq, see review (53). The majority of studied sRNAs function *in trans* and have more than one target and the chromosomal locations of the target genes are not linked. Moreover, they typically require the RNA-chaperone Hfq, to bind to their target mRNAs. A model as to how sRNA cycles on and off Hfq has been proposed (54); which speaks to its significance. Interestingly, *Pg* is an Hfq-negative organism. Although the binding of HU proteins to RNA is only beginning to be investigated, HU has been shown to bind sRNAs in *E. coli* (55), so it is possible that HU-like proteins play an Hfq role in *Pg*. **Importantly, antisense RNA (asRNA) molecules are by far the most abundant transcripts in the bacterial cell (reviewed in (56, 57); yet their characterization lags behind that of sRNAs.** The size of asRNAs has a wide range (~100 - 7,000 nucleotides) and the abundance of these molecules can vary from barely detectable to high levels. Moreover, depending on function, they can be transcribed at the same time or under opposing conditions as the sense strand (56).

Synthesis of sphingolipids (SLs) by *Pg* influences the presentation of capsule. In eukaryotes, SLs not only serve as structural components of membranes they also form lipid rafts, providing energetically favorable microdomains capable of stabilizing select membrane proteins (58) and synthesis in eukaryotes is well described (59, 60), yet the pathway in bacteria is still under investigation. As shown in Fig 1, in all organisms the first step is the synthesis of a sphingoid base by the rate limiting enzyme serine palmitoyltransferase (SPT; PG1780), followed by the biosynthesis of ceramides (attachment of an amide linked fatty acid) and finally, formation of complex SLs (through the attachment of head groups to C1 of the sphingoid base). SL synthesis by bacteria is rare and, for the most part, restricted to human commensals belonging to the phylum Bacteroidetes (61); which includes many of the Gram-negative anaerobes that persist in several anatomical niches of the human host such as *Bacteroides* species in the intestinal tract, and *Porphyromonas*, *Tannerella*, and *Prevotella* which persist in the oral cavity, primarily below the gingival margin (62-64). Studies to determine the function of bacterial SLs are limited. It has been shown that synthesis of SLs is central to survival during stationary phase and for resistance to oxidative stress and to form membrane

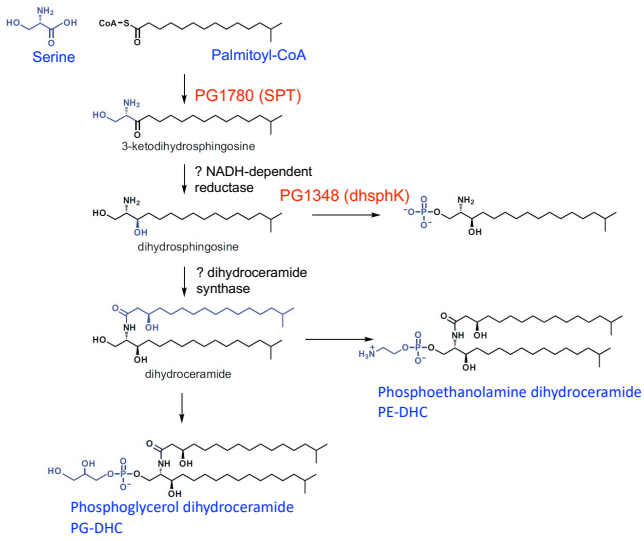

Fig 1. Predicted pathway for sphingolipid (SL) synthesis in Pg. Phosphorylation of dihydrosphingosine by PG1348 diverts this key substrate away from the synthesis of SLs (PG-DHC and PE-DHC). Deletion of PG1780 (serine palmitoyltransferase; SPT) results in an SL-null strain.

microdomains similar to their eukaryotic counterparts (65-67). Moreover, recent studies have shown that these host-like lipids play a role in microbiome-host homeostasis (66-71). Most relevant to this research program, our group determined that SL synthesis is required for the presentation of A-LPS and K-antigen capsule on the cell surface of *Pg* strain W83, serotype K-1 (66), and this finding aligns with our discovery of a matching asSuGR target sequence in the PG1780 (SPT) operon, suggesting that synthesis of surface glycans and SLs are coordinated by a global regulatory system. Our working model is that SLs play a role by either positioning proteins assemblies in the membrane for synthesis of this complex polysaccharide and/or a subset of SLs may play a role in anchoring capsule to the outer membrane. To increase our understanding of the function of SLs in relation to surface glycans, we have been generating mutant strains in genes within operon predicted to be involved in SL-synthesis and determining the effect on surface polysaccharides. We have published our characterization of an SL-null/SPT (ΔPG1780) mutant strain (66, 72, 73), and our characterization of PG1348 a novel dihydrosphingosine kinase (*dhsphK)* (74), showing that the *ΔdhsphK* mutant is defective in the presentation of K-antigen capsule. Since the SPT-PG1780 locus has a copy of asSuGR (see Fig 4) and synthesis of SLs positively influences the presentation of surface glycans, we are proposing to determine the link between asSuGR and expression of genes in the SPT-PG1780 locus.

Impact of this research program. Little is known about the molecular mechanisms that regulate the production of *Pg* capsule or if its synthesis and the presentation of other cell surface structures is coordinated. This gap in knowledge limits our understanding of *Pg*'s pathogenic potential. Until the mechanisms that control capsule expression are determined, methods toward hypothesis-driven therapeutics against the virulence and dissemination of *Pg* and its subsequent role in periodontal and other systemic diseases are limited. Although there is much to learn about the function of HU PG0121 and HU PG1258 in *Pg*, we postulate that these NAPs play an essential role in controlling the switch to a pathogenic state. Based on published and new data described below, these two NAPs may provide therapeutic targets to undermine *Pg* virulence beyond regulating K-antigen expression. Furthermore, for *Pg* to persist as a human commensal it must readily adjust to changing environmental conditions. We propose that NAPs working in concert with asRNAs and RNA processing enzymes, represents an exquisite and energy-efficient strategy for making these adjustments. The progress in identifying and characterizing sRNAs has made it clear that sRNAs are pervasive and likely exceed protein regulators in number and diversity. More in-depth knowledge is required to fully understand how regulatory RNAs control their targets and how they are coordinately expressed, cycled, and how they localize their targets, in particular in organisms like *Pg* that lack Hfq. In addition, although it is well documented that heme is a key signal for Pg, how Pg senses heme remains a gap in knowledge. These studies will characterize a novel heme sensor, which is critical to Pg survival and virulence.

(B) INNOVATION

The innovation in this proposed research is four-fold. (1), we are unraveling a complicated regulatory mechanism that controls key virulence determinants in *Pg*; (2), we have discovered novel DNA-binding proteins belonging to the DNABII family that control these virulence factors; (3) we are proposing to characterize a long (504 bp) non-coding antisense regulatory RNA at the functional level that is encoded within a novel 77 bp inverted repeat element (77bpIR); and (4) we are deciphering activation of a two-component sensor, which is critical for heme/iron acquisition and synthesis of the K-antigen capsule. The first indication that PG0121 and PG1258 are novel was their high sequence similarity to HU protein, yet their lack of key amino acids (*E. coli* consists of NPQT, where the proline is crucial for DNA binding, whereas PG1258 and PG0121 contain NISK and NPKT, respectively) that are known to play a functional role in their interaction with DNA. In addition, there is an unusual lack of reactivity to DNABII antisera (unpublished data). Our studies have shown that unlike other DNABII proteins, PG1258 does NOT seem to bend DNA. It would be the first member of the family that does not. PG1258 appears to bind DNA in a sequence-specific manner indicating that it has functional properties more similar to IHF, making it a novel DNABII nucleic acid-binding protein. Regarding our proposed characterization of asSuGR, despite the high and still increasing number of regulatory RNAs being identified, only a small proportion of them have been analyzed at the functional level. Given recent findings that antisense RNA synthesis is pervasive in the bacterial cell, asRNAs could have a significant, yet largely unexplored, impact on gene regulation and cycling of nucleic acids, therefore we are proposing a detailed characterization of this novel regulatory RNA at the mechanistic level. Lastly, our plan to elucidate the ligand/signal that activates the two-component system (PG0719-PG0720) is part of our innovative approach to better understand Pg's pathogenic potential.

Preliminary Studies.

Characterization of PG0121 and PG1258. We have shown that PG0121, which is located at the 3'-end of the K-antigen capsule locus (shown in Fig. 2) is transcriptionally linked to the capsule operon (16). As noted, PG0121 is predicted to be HUß, a member of the DNABII family of proteins. We have assessed both the *in vitro* and *in vivo* functional characteristics of PG0121. *In vitro*, we discovered that PG0121 binds to various DNA substrates (75). *In vivo,* PG0121 expressed ectopically in an *E. coli* HU deficient background (*hupAhupB)* was able to complement several phenotypes including low pH sensitivity and filamentation, demonstrating that PG0121 was capable of canonical DNABII functions (17). We also confirmed that PG1258, the predicted HUα sub-unit, is essential (16), which is supported by another study (76). In addition, using DNase foot printing, we compared the binding of PG0121, PG1258, both proteins equilibrated together, and *E. coli* IHF to a *bona fide* IHF binding site from bacteriophage lambda (H' from the prophage *att*L locus) and confirmed that both the *E. coli* IHF and PG1258 provide protection centered around the known consensus IHF binding sequence (TATCAATTTGTTG) while PG0121 bound less efficiently (for space considerations, data not shown). These results show that PG1258 is more IHF-like than HU-like, making it a novel DNABII protein**.** Importantly, equilibration of PG0121 and PG1258 together resulted in a weakened affinity and specificity compared to PG1258 alone. The combination of equilibrated PG0121 and PG1258 seems to weaken the footprint, consistent with PG0121 forming either non-productive interactions at the protein-protein or protein-DNA level.

DNABII proteins act as both homo and heterodimers. We have shown that PG0121 readily forms homodimers *in vitro* (75). In *E. coli* the HUα and HUß subunits form both homo and heterodimers with respect to one another where each dimer species has different DNA binding properties and apparent functions (77). When Pg is treated with 0.1% of the crosslinking agent, glutaraldehyde, PG1258 forms abundant dimer bands suggesting that the native state of PG1258 is a dimer. When incubated together prior to crosslinking and immunoprecipitation (78) with anti-PG1258 serum, PG1258 and PG0121 form a heterodimer band when visualized with Western blot analysis using anti-PG0121 serum (data not shown). These results indicate that PG0121 and PG1258 interact and form heterodimers *in vitro*, but whether they function as heterodimers *in vivo* remains to be determined. We will actively pursue this subject in sub aim 2.2. Importantly, we have identified an IHF binding site just upstream of the 77bpIR element (CATCAATGGCTTG). Since PG1258 displayed protection in a manner similar to that of IHF, yet equilibration of PG0121 and PG1258 together resulted in a weakened affinity and specificity compared to PG1258 alone, our working model is that **PG0121 activates K-antigen expression by alleviating direct binding and early transcriptional termination via PG1258 (see Fig. 2).**

As shown in Fig 2, the 77bpIR element is located at the 5' end of the K-antigen capsule locus between PG0104 and PG0106. We have shown that HU PG0121 up-regulates the transcript levels of this operon (16, 17, 75), and that the 77pbIR element deletion mutant not only produces less K-antigen capsule, it is also altered in LPS synthesis (79). The phenotype was complemented when the mutation was restored on the chromosome, however the 77bpIR element did not complement when provided on a plasmid *in trans*; indicating that the 77bpIR element is, at least in part, *cis*-acting. Using RNA-seq data, qPCR, and 5'-3' RACE analysis we delimited an asRNA molecule (asSuGR) encoded within the 77bpIR element. To explore its function, we generated a *Pg* strain W83 harboring a plasmid containing this region and showed that it is enhanced in capsule and LPS synthesis (23), indicating that this segment of DNA is also *trans*-acting. As shown in Fig 2, our working hypothesis is that processivity *i.e.,* the uninterrupted transcription by RNA polymerase, is a challenge for transcription of the large capsule operon transcript on the sense strand; therefore, transcription and processivity are regulated via a mechanism of antitermination. The data indicate that asSuGR along with PG0121 (HU-β) support processivity and synthesis of the capsule operon. In addition, asSuGR may also bind to the sense transcript and promote stability. While exploring regulation of asSuGR, we identified a highly conserved σ54 consensus sequence (TGG-N9-TGC) within the coding region of asSuGR, suggesting that a σ54 response regulator binds this site. We are proposing to follow-up on this finding (Aim 1.1). Further, a study was published showing the regulon of the two-component response regulator PG0720 (PGN_0753 in strain 33277) (80), and we noted that genes adjacent to other copies of asSuGR on the chromosome were differentially expressed. We therefore followed-up on this discovery and determined that PG0720 does indeed activate expression of asSuGR from a promoter within the 77bp sequence. This led to our current working model that PG0720 indirectly influences transcript levels of the capsule operon expressed from the sense strand. Our studies also showed that deletion of PG0720 confers a defect in the presentation of surface glycans compared with the parent strain and quantitative RT-PCR (qPCR) analysis determined that the overall expression of genes involved in capsule synthesis were down-regulated in the PG0720 mutant (23). Lastly, the PG0720 deletion mutant showed reduced virulence. Importantly, RNA-Seq analysis showed that the expression genes involved in iron acquisition are down-regulated

in the ΔPG0720 mutant compared to the parent strain (23). This finding aligns with the previous study on this two-component system mentioned above which showed that PG0720 (PGN_0753) controls a suite of genes involved in acquisition and uptake of iron/hemin and the system was designated HaeSR (for hemin) (80). Given this published information, **we hypothesized that heme availability is a key signal that influences this two-component system and our preliminary data shows that the sensor component of this system (PG0719) interacts with heme.** Altogether, our studies have determined that asSuGR is a cis- and trans-acting antisense RNA molecule involved in regulating the production of Pg surface glycans and its expression is at least in part controlled by the two-component system PG0719-PG0720.

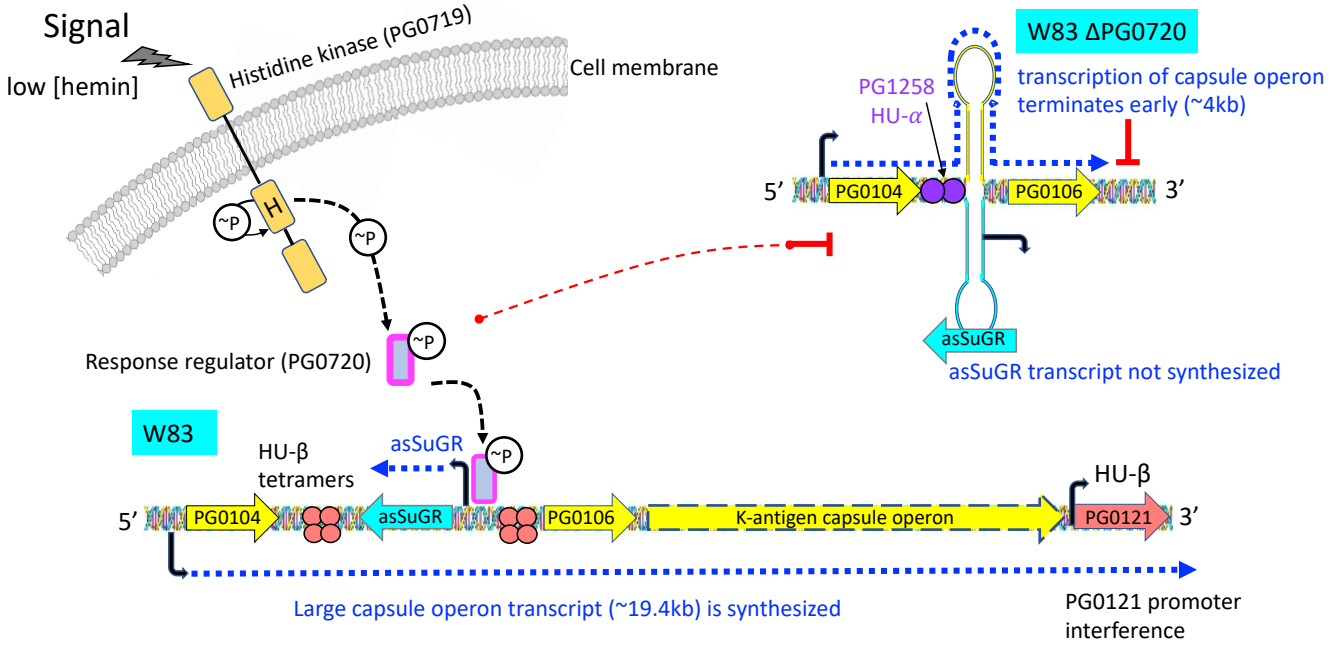

Fig 2. Proposed working model describing the impact of transcription of asSuGR and PG1258 repression on transcription of the K-antigen capsule operon on the sense strand. When the two-component sensor kinase (PG0719) senses low levels of hemin, it autophosphorylates and then transfers the phosphate to its cognate response regulator PG0720. Phosphorylated PG0720 activates transcription of asSuGR. When asSuGR is transcribed (W83) the large capsule operon transcript (~19.4 kb) on the sense strand is synthesized and this interferes with activation of the PG0121 promoter. When asSuGR is not transcribed (ΔPG0720 or repression by PG1258 homodimers) synthesis of the large capsule operon is terminated earlier.

(C) APPROACH: EXPERIMENTAL DESIGN AND METHODS

Aim 1. Determine how the 77bpIR region encoding asSuGR regulates the levels of surface glycans.
Rationale: We have shown that transcription at the 77bpIR regulatory element is bi-directional, and we have delimited the transcription of asSuGR mRNA. We have also determined that when asSuGR is expressed by *Pg* from a plasmid, this alters both K-antigen capsule and LPS synthesis; indicating that asSuGR acts *in trans*. Importantly, there are a total of eight matching asSuGR targets on the chromosome, suggesting that the asSuGR produced from the 77bpIR element influences global gene expression. Moreover, since the SPT-PG1780 locus has a copy of asSuGR (see Fig 4) and synthesis of SLs positively influences the presentation of surface glycans, we are proposing to determine the link between asSuGR and expression of genes in the SPT-PG1780 locus. As discussed in preliminary studies, our working model is that asSuGR along with HUβ support processivity and synthesis (and/or stability) of large transcripts (designated here: the capsule operon and the SPT-PG1780 operon). The goals of this aim are to determine if asSuGR promotes transcription (and/or stability) of transcripts that are generated from these two loci and to continue our efforts to identify other regulatory proteins that interact with the 77bpIR element.

1.1 Determine the role of the 77bpIR region in the regulation of glycan synthesis. To determine the role of the 77bpIR element in regulation, we need to better understand the regulation and function of asSuGR. In this sub-aim we will determine the sense and antisense transcript levels during different phases of growth with and without heme, while determining the effect of PG0121 and PG0720 as well as other regulatory proteins on expression of the capsule operon and genes in the PG1780-PG1788 locus.

Transcriptional analysis of the capsule locus (PG0104-PG0121) and the SL-synthesis locus (PG1780-PG1788). Northern blot analysis with riboprobes specific to the sense and antisense transcripts will be used, as well as RT-qPCR, to examine when asSuGR and sense strand mRNAs are up- or down-regulated. To perform these experiments, we will grow *Pg* to early, mid, and late exponential, as well as late stationary phase of growth (comparing heme deplete and replete conditions), isolate RNA and do Northern analysis, as previously described (14, 16, 17). We will also continue to perform strand specific qPCR to evaluate bi-directional transcription within the capsule operon and the PG1780 locus (SL-synthesis). In parallel, we will examine the asSuGR over expressing strain (pT-HP); (23)) to the WT with the empty plasmid (control), to evaluate whether or not over-expression of asSuGR influence the levels of different transcripts. In parallel, we will study transcript levels in regulatory mutants. Since we have shown that the response regulator PG0720 is involved in regulating the transcript levels of genes in the capsule operon, we plan to focus on determining the expression levels in the ΔPG0720 mutant. In addition, since we have identified a highly conserved σ54 consensus sequence (TGG-N9-TGC) within the coding region of asSuGR, we will examine the impact of sigma 54 (σ54) response regulators. Importantly, unlike σ70-type sigma factors, which can spontaneously separate double-stranded DNA and initiate transcription after forming the RNAP holoenzyme, σ54 is incapable of transitioning from the closed complex to the open complex on the DNA without the assistance of an ATP-hydrolyzing response regulator, therefore we hypothesize that one of the σ54 response regulator is required. The following mutants will be examined by Northern and RT-qPCR analysis: W83ΔPG0121, W83ΔPG1105 (σ54), W83ΔPG0747 (σ54 response regulator), W83ΔPG0016 (σ54 response regulator), and W83ΔPG0386 (a predicted σ54 modulation protein). Importantly, these regulatory genes are not predicted to be essential (76); except PG1105, however, since σ54 is not typically essential this essentiality may be conditional, so we will try and generate a PG1105 deletion mutant in rich medium under strictly anaerobic conditions. We will also characterize the phenotype of select regulatory mutants that show a defect in transcription in the capsule locus by examining the surface polysaccharide composition, growth rate, stress response (e.g., resistance to oxygen stress or hydrogen peroxide stress), and RNA-Seq analysis using our established methodology (16, 23, 66, 72, 73, 79, 81). In addition, we will use the *Galleria mellonella* (greater wax moth) larvae model as a first step in assessing the virulence of these glycan-altered mutants, using an established methodology that has been used to evaluate Pg virulence in our lab and by other researchers in the field (23, 81-83).

1.2 Pull down assays. In a complementary approach, pull down assays will be used to identify additional regulatory proteins that interact with the 77bpIR region. We have been working to optimize a protocol adapted from Jutras *et al*., 2012 (84). In general, the DNA sequence of interest is affixed to beads, and then incubated with bacterial cytoplasmic extract. Washes with buffers containing nonspecific DNA and low-salt concentrations are used to remove non-adhering and low-specificity DNA-binding proteins, while subsequent washes with higher salt concentrations elute more specific DNA-binding proteins. Eluted proteins are then identified by standard proteomic techniques. As shown in Fig 3, to perform these experiments, we have been mechanically lysing Pg and then taking the cytosolic fraction and incubating it with dynabeads that are coupled to the DNA 77bpIR element probe (HP) to allow protein-DNA binding. Herring sperm is added to restrict non-specific binding and a random region from within the capsule locus that is also 1408 bp is used to generate a control probe (CT).

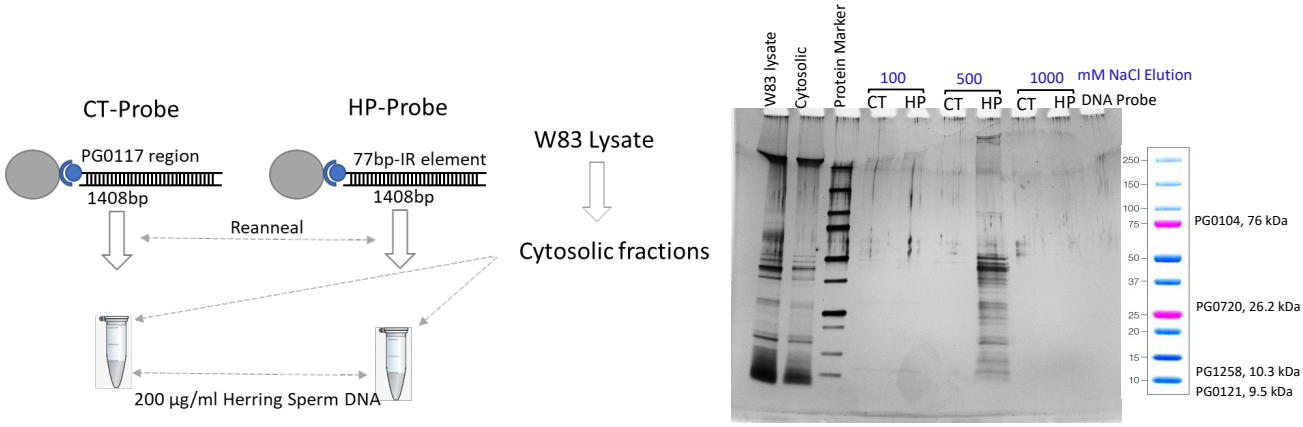

Fig.3. DNA-affinity pull down assays. Cytosolic fractions of Pg strain W83 lysates were incubated with a 77bpIR probe (HP) and a control DNA probe (CT). Herring sperm (200 µg/ ml) was added to restrict non-specific DNA-binding. Silver staining of eluants shows that a variety of proteins elute in the 500mM wash. Indicated next to the molecular weight markers are proteins predicted to interact with the 77bpIR region probe.

A gradient of sodium chloride (100, 300, 750, and 1000mM) is then used for elution and the protein bound to the probe is analyzed by silver staining. Our preliminary studies show that proteins are not eluting in the 100mM wash, however a number of proteins elute with the 500mM wash. We are currently repeating these experiments and using Western blot for PG0720, PG0121, and PG1258 along with mutant strains to validate our results and protein sequencing to identify additional proteins that interact with this element. We predict that this approach will pull down a sigma 54 response regulator and potentially PG0104 (a predicted topoisomerase encoded at the 5' end of the capsule operon) as well as PG0720, PG1258 and PG0121. The identification of these regulatory proteins and additional protein-DNA interaction studies combined with information obtained in Aim 2 will be used to build a model as to how transcription of the 77bpIR element is regulated.

1.3 Determine transcriptional linkage of genes in the SL-synthesis locus. We identified a gene (PG1780) encoding the enzyme serine palmitoyltransferase (SPT), generated a deletion mutant (W83 ΔPG1780), and showed that the mutant was unable to synthesize SLs (66). This was the first SL mutant generated in Pg. As shown in Fig 4, the PG1780 locus contains at least six genes and harbors a large intergenic region between PG1786 and PG1788 whose sequence is an exact match to asSuGR. Our working hypothesis is, since asSuGR2 lacks the 77bp promoter, this site represents a target for the asSuGR molecule produced in the capsule operon, ultimately supporting transcription (and possibly stability) of a PG1780-PG1788 transcript, which is predicted to be at least 8,460 kb. Testing of this hypothesis is proposed above in sub-aim 1.1. Preliminary data indicates that PG1786 is transcriptionally linked to PG1784 and PG1788 (data not shown). Here, we are proposing to continue to survey the operon structure by hybridizing with probes from each of the open reading frames and use RT-PCR to confirm transcriptional linkages of the genes within the locus. In addition, we have already generated deletion mutants of asSuGR2 and PG1784 and our plan is to further analyze the region by continuing to make non-polar deletion mutants of genes in this locus and compare transcription of the mutants to the parental strain, using our established methodology (16, 23, 66, 72, 73, 79, 81).

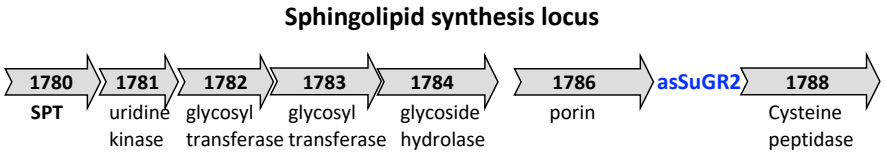

Fig 4. Schematic representation of the genes located in the PG1780- PG1788 locus.

1.4 Evaluate RNA stability. To determine if asSuGR impacts RNA stability, we will study the kinetics of synthesis and decay of sense and antisense transcripts using Click-iT technology (Life Technologies). The Click-iT method is based on the bioorthogonal click chemistry reaction, where ethynyl uridine (EU) is incorporated onto RNA during synthesis. Biotin can then be "clicked" onto the RNA strand and streptavidin magnetic beads can then used to capture nascent RNA. Although this technology has primarily been employed to study mammalian cells, this EU labeling has been validated in *Listeria* (85). In brief, we will use EU-labeling to perform pulse/chase experiments. For these analyses, *Pg* strains will be grown to early exponential (OD_{550} of 0.3) or late exponential (OD_{550} of 0.9), at this point the cells will be "pulsed" with 1mM EU and grown for 6 hr (approximately 2-doublings) in EU containing medium. The cells will then be "chased" by pelleting, followed by re-suspension in EU-free, pre-reduced medium. Cell samples will be collected over 60 min and RNA will be isolated, as previously described (16, 17), and then captured using the Click-iT capture kit, following manufacturer's instructions. Four different time points, including the reference sample (just before the chase), will be analyzed simultaneously by RT-qPCR, as previously described (16, 17). Degradation will be considered to become the major phenomenon responsible for lowering EU-tagged mRNA levels. To initiate these studies, we will examine the effect of over expression of asSuGR on stability of large capsule operon transcript, followed by examination of the PG1780 operon. We predict that asSuGR plays a role in stabilizing these large operon transcripts.

Aim 1. *Expected Outcomes Potential Pitfalls and Alternative Approaches.:* This aim is a direct continuation of our work to provide a better understanding of how the 77bpIR element regulates gene expression. In general, no significant pitfalls are anticipated as the proposed methods and developed resources are well established (14, 16, 86-88). Data obtained from these studies will build upon our knowledge of the regulatory pathways that control expression of key virulence determinants in *Pg,* including capsule, LPS, and potential sigma 54 controlled regulatory pathways, which are often responsible for generating rapid responses to environmental change (89, 90) and are currently understudied in *Pg.* Our working model is that asSuGR directs stabilization of the capsule operon. This hypothesis may of course prove not to be correct. We may discover that the complementary interaction enhances termination, and thus attenuates expression; however, the proposed experiments are designed to support or refute our hypothesis and will provide the required information to determine the underlying

mechanism. If the data support the hypothesis that asSuGR enables transcriptional linkage between PG1784 and PG1788, then the predicted porin encoding gene at the 3' end of the locus (PG1786) may play a central role in membrane biogenesis, and we will investigate this porin in more detail. To complement the genetic approach, we are also proposing to use DNA affinity (pull down assays) to identify additional proteins that interact with the 77bpIR region.

AIM2. Characterization of *P. gingivalis* DNABII proteins (PG0121 and PG1258).
Rationale: our studies have shown that the DNABII protein PG0121 plays a critical role in capsule expression and that PG1258 which is essential for *Pg* survival, interacts with PG0121 and binds DNA with sequence specificity (IHF sites). Thus here, we propose to tease out the independent and cooperative functions of PG0121 and PG1258 on K-antigen capsule expression using *in vitro* (Aim 2.1) and *in vivo* systems (Aim 2.2). All experiments outlined in this Aim will proceed in tandem.

Aim 2.1 Specificity of PG0121 and PG1258 for K-antigen specific locus interactions and canonical IHF binding sites. As previously mentioned, DNABII proteins are a homologous family of proteins of highly similar primary and secondary structure that are comprised of two forms, HU and IHF. While HU protomers appear to bind DNA in a sequence independent fashion, IHF protomers (both homodimers and heterodimers) (29-33) bind to specific sequence sharing the consensus WATCAANNNNTTR (where W is A or T, N is any nucleotide and R is A or G (34)). Here we will examine *in vitro* interactions of PG0121 and PG1258 with the upstream regions of the K-antigen operon, with other potential binding sites in the chromosome of *Pg* as well as *bona fide* canonical IHF binding sites. Importantly we will also evaluate their independent and cooperative HU and IHF functions.

Biacore analysis of 77bpIR binding sites and predicted IHF binding sites. We have presented in our Preliminary Data that PG1258 specifically binds the 77bpIR sequence, while we have published that PG0121 likewise has specific affinity for the same regions albeit with very different complexes formed with each protein. Here we will examine the same DNA substrates (75) using surface plasmon resonance (SPR; using a Biacore T200) and determine how PG1258 binding compares to PG0121. This will determine if one subunit has a preference for binding to the 77bpIR. In addition, we will bind equimolar amounts of each protein, equilibrated with one another (>24hrs)(91), as well as added the proteins simultaneously to initiate the binding reaction to determine if the proteins 'interact' to change their net interaction with the substrate. In parallel and identically, we will also examine both proteins separately as well as together in quantitative EMSA where we examine the IHF binding site that we have identified upstream of the 77bpIR element. Our preliminary studies determined that PG0121 and PG1258 separately footprint the IHF sites. Again, both individual and cooperative binding affinities will be evaluated.

Binding to sites identified in silico and by ChIP-seq. We will use information garnered from BLAST (preliminary studies; see Aim 2.2) and ChIP-seq analysis (Aim 2.2) to identify binding sites on the *Pg* chromosome for PG0121, PG1258 and a 1:1 mixture of equilibrated and non-equilibrated PG0121 and PG1258. In particular, we will focus our attention on the 77bp regions. Once identified, the top 20 matches will be PCR amplified into 100 bp DNA amplicons with the match to consensus centered in the DNA fragment. These DNAs will then be used in SPR experiments described above to quantify their binding affinity. Five randomly selected adjacent 100 bps that fail to have a match to the consensus sequence(s) will be used as controls. While ChIP-Seq is a powerful technique for identifying nucleoprotein interactions under predetermined conditions, even the most informed conditions do not necessarily cover all possible interactions throughout the life cycle of the bacterium, therefore studies on *in silico* identified targets that are not detected with ChIP-Seq are warranted.

PG0121 and PG1258-RNA interactions, finding specific targets vs secondary structure. Here we will further examine the interaction of the DNABII proteins and determine the extent of their specificity for the upstream mRNA region of the K-antigen operon, along with asSuGR. We will focus on multiple RNA substrates that include and exclude the IHF binding site. RNAs to be tested will include, the 150 base region just upstream of the first 77baseIR, 100 base region including the first 77base IR, 400 base region that includes up to the second 77base IR and finally the two 77IRs base paired together without any other RNA present. Proteins to be tested will be PG0121, PG1258 and the PG1258-PG0121 complex. After this baseline analysis, identical experiments will be performed with the asSuGR RNA, which has its own internal 32bpIR, to determine if this RNA species plays a role in DNABII binding and function. As a control, we will use yeast tRNA because of its known secondary structure to determine the level of specificity of each DNABII combination.

Aim 2.*2 In vivo* characterization of PG0121 and PG1258. Our discovery that PG1258 binds site specifically to a predicted IHF sequence upstream of the 77bpIR and that PG1258 and PG0121 interact as judged by crosslinking and IP suggests a paradigm shift in how these two DNABII proteins function *in vivo.* Here, we will

examine the steady-state levels of proteins *in vivo* as well as the likelihood that they will interact *in vivo*. We will also perform ChIP-Seq analysis to study the interactions of these proteins with the entire *Pg* genome. This will complement the *in vitro* binding experiments above.

Steady-state levels of PG0121 and PG1258. In *E. coli*, the protein levels of the two HU subunits vary during growth phase (92). Preliminary western analysis indicates that the level of HU PG0121 is elevated during exponential growth phase and then decreases as the cells enter stationary phase (data not shown). As a prelude to examining interactions of PG0121 and PG1258 *in vivo,* we will further examine the steady state levels of each protein under various growth conditions, specifically different phases of growth in complex rich medium with high (5ug/ml) and limiting (1ng/ml) levels of hemin. We are examining the effect of availability of hemin, since we have previously determined that HU PG0121 has a strong impact on gene expression under iron limiting conditions (17). *Pg* will be grown as previously described and cells will be isolated during early-, mid-, and late exponential phase to cover the classic phases of growth and we will perform quantitative immunoblot analyses (93) using antisera to either PG1258 or PG0121. In parallel, we will repeat these experiments with our PG0121 deficient strain. Information obtained from these experiments will facilitate the ChIP experiments, where we examine PG1258 and PG0121 interactions *in vivo*. We will also use the conditions above and perform crosslinking on live cells followed by IP. IP will be performed with either antiserum to PG0121 or PG1258 (pre-bleed serum will be used as a control). Both subunits are easily separated by urea-triton PAGE. Information obtained from these experiments will facilitate the ChIP experiments, where we examine PG1258 and PG0121 interactions *in vivo*.

Independent and cooperative interactions of PG0121 and PG1258 with the chromosome of Pg. Here, we will utilize chromatin immunoprecipitation (ChIP) followed by high-throughput sequencing (ChIP-Seq) to map the *in vivo* association sites of DNABII proteins encoded by PG0121 and PG1258. This will allow us to study the dynamic interactions of these proteins with the entire genome. ChIP-Seq has previously been used successfully to identify the chromosomal locations at which regulatory proteins are found in *Pg (80, 94)* and by Dr. Ramsey in other bacteria (95-97). **It is important to note that we have already generated specific and mutually exclusive antibodies to each of these DNABII proteins, therefore this analysis can be performed by immunoprecipitating nucleoprotein complexes with each antibody.** In brief, to identify DNA targets, we initiate our studies by growing *Pg* strain W83 and the ΔPG0121 mutant to early exponential and late exponential phase of growth. *In vivo* cross-linking will be initiated with the addition of formaldehyde and quenched with the addition of glycine. The cells will then be harvested, washed, and lysed, after which DNA will be sheared by sonication to an average size of 500 to 2,000 bp (78). Cell debris will be removed by centrifugation and the cleared supernatant will be used as the **input sample**. An aliquot of the input sample will be incubated with Ultralink protein A/G beads (Pierce) and either antibodies to PG0121, PG1258, or pre-bleed serum IgG. The beads will be collected with Spin-X centrifuge tube filters (VWR), washed, and the IP complexes will be eluted. IP samples will be un-cross-linked and the DNA eluted. Western blot analysis will be used to confirm precipitation of the DNA-binding protein. The **output DNA** will then be prepared for sequencing using Illumina technology using the NEBNext ChIP-Seq Library Prep Reagent Set for Illumina (New England Biolabs), according to manufacturer's protocol. The libraries will be run on a 2% agarose gel and 0.25 –0.50 kb fragments will be selected. NEBNext Multiplex Oligos for Illumina (NEB) will be used to PCR amplify the purified fragment and the PCR products will be purified. Sequencing will be performed using a NovaSeq 6000 platform. ChIP-seq data will be mapped to the *Pg* genome using our established protocols. The libraries will be analyzed with GenomeView to identify promoter regions. We will validate the top six association sites using mobility shift assays, and evaluate them for binding affinity by SPR using PG1258, PG0121 and a 1:1 mixture of PG1258 and PG0121 (equilibrated and non-equilibrated) (17, 75). This will both biochemically verify the results of the ChIP-Seq and further help distinguish the potential interactions and targets of PG1258 and PG0121. The PG0121 null strain will serve as a control with PG0121 antibody and also determine if there is any change in sequences that are immunoprecipitated with the antibody to PG1258. The pre-bleed serum experiment will provide a mock immunoprecipitation control for all experiments. In this way, we will determine if PG0121 and PG1258 are competing for the same DNA sequences or more likely interacting to bind to the same sequences.

Aim 2. *Expected Outcomes Potential Pitfalls and Alternative Approaches*.: In Aim 2.1, the interaction of PG1258 with the IHF site, the likely interaction of PG1258 and PG0121 and their respective interaction on DNA will be examined thoroughly by multiple methods. Definitive outcomes are assured in all the experiments with the possible exception of ChIP-Seq where chosen conditions for crosslinking will strongly affect the outcome. In this regard, determining steady-state levels and some initial IP experiments should be completed be completed first in Aim 2.2, to facilitate choosing *Pg* growth conditions for ChIP-Seq. If initial IP experiments with specific

antibodies are not successful, the DNABII proteins will be modified to include an epitope tag to be used for IP, as in (98). Second, it is also possible that the ratio of PG1258 and PG0121 varies at different phases of growth, as it has been shown for other DNABII family members that otherwise interact (92, 99). Should a constant ratio of PG0121 and PG1258 other than 1:1 persist throughout most growth conditions, we will repeat the experiments in Aim 2.1 with this new ratio. Finally, binding affinity experiments with the various RNAs, including asSuGR, and their specific K_ds will better determine how competitive a native duplex DNA sequence is compared to its corresponding duplex RNA. The actions of the DNABII family at this and other promoters have proven to be more complicated than a single protein binding to a DNA sequence. This Aim will elucidate the means of PG0121 and PG1258 in regulating expression from the 77bpIR region.

AIM 3. Heme sensing by the two-component sensor PG0719.

Rationale: Recent reports have shown that the PG0719-PG0720 two-component system controls expression of genes involved in heme acquisition (39) entry into endothelial cells (23, 100) and expression of asSuGR (23), which is the focus of Aim 1. Exploring the possible interaction of PG0719 with heme (as well as its degradation byproducts), at the protein level, can provide direct evidence into the system's activation signal and insights into the underlying mechanism directing this molecular switch. The goal of this aim is to identify and characterize the activation signal or metabolites sensed by PG0719 at the atomic level. In particular, since bleeding on probing is a clinical hallmark for periodontitis and Pg has a variety of mechanisms for lysis of red blood cells, we have focused on metabolites released from erythrocytes, in particular heme (101-108). In addition, we aim to probe and decipher the conformational changes associated with signal transduction within this signaling pathway to obtain the desirable mechanistic insights.

Aim 3.1 Overexpression and Purification of Functional PG0719. PG0719 is predicted to adopt the fold of a sensory histidine kinase (~50 KDa). This segmented and modular fold gives rise to a small sensory periplasmic sensory domain (~13 KDa), flanked by two transmembrane helices and a larger cytoplasmatic transducer kinase module (~30 KDa). In this sub-aim, we aim to overexpress and purify the *(a)* full-length PG0719 as well as its individual domains, including *(b)* the periplasmic sensory domain and *(c)* the cytosolic kinase module required for downstream biochemical and biophysical analyses. First, the different protein constructs will be subcloned into pET28 or pET41 expression vectors where they will be each conjugated in frame to a cleavable affinity tag (such as a poly-Histidine tag) at its N- or C-termini. We will then screen for different conditions to allow optimal overexpression levels in *E. coli*. Once optimal expression conditions are identified, we will establish a purification scheme for each construct. Notably, for the full-length membrane spanning PG0719 protein, we will also screen for suitable detergents promoting adequate protein extraction and solubilization, while for the soluble domains this step will be omitted. The three different protein constructs will be then purified by affinity, charge and size-based chromatography. Protein purity and identity are assayed by native and denaturing PAGE, tandem mass spectrometry (MS/MS) and peptide fingerprinting. The purified detergent-solubilized PG0719 or the soluble kinase domain will be tested for their auto- and trans-phosphorylation activity via an established assay (109) with Phos-tag for detection (Wako). For this assay, we will also use the purified PG0720 response regulator obtained in our previous studies (23). In addition, we will clone, express, and purify a PG0719 phosphorylation deficient mutant (H226A – catalytic histidine) to serve as a negative control for this functional phosphorylation assay *in vitro*. So far and as a preliminary result, we have established an expression and purification protocol for the soluble sensory domain resulting in >95% purity (See Fig 5A).

Aim 3.2 Characterize PG0719's interacting metabolites. Protein sequence analysis allowed us to identify a conserved PC pair motif (Proline103-Cysteine104) associated with heme binding at PG0719's periplasmic sensory domain (110), providing a clue toward a potential activation signal of PG0719. Our preliminary qualitative binding assay further supported this hypothesis by revealing that the purified PG0719 periplasmic sensory domain can irreversibly bind to heme-coated-agarose beads (Fig. 5A). Taken together and in line with our previous findings (23), available literature (12, 80, 111) and predicted-fold similarity to other sensors (38), we will screen for potential interacting metabolites, in particular heme and its degradation products, biliverdin, bilirubin and protoporphyrin IX. We will use *UV-Vis absorbance spectroscopy* as a powerful technique to characterize the binding of absorbing metabolites to PG0719. When heme, or its degradation products, binds to a protein, it alters its unique UV-Vis absorbance spectrum, leading to shifts in absorbance peaks (112). Subsequent metabolite-protein titrations, leading to gradual alterations in peak intensities, can be further used to quantify the amount of both free- and bound-metabolites, and provide the specific binding parameters. If binding is observed, comparing

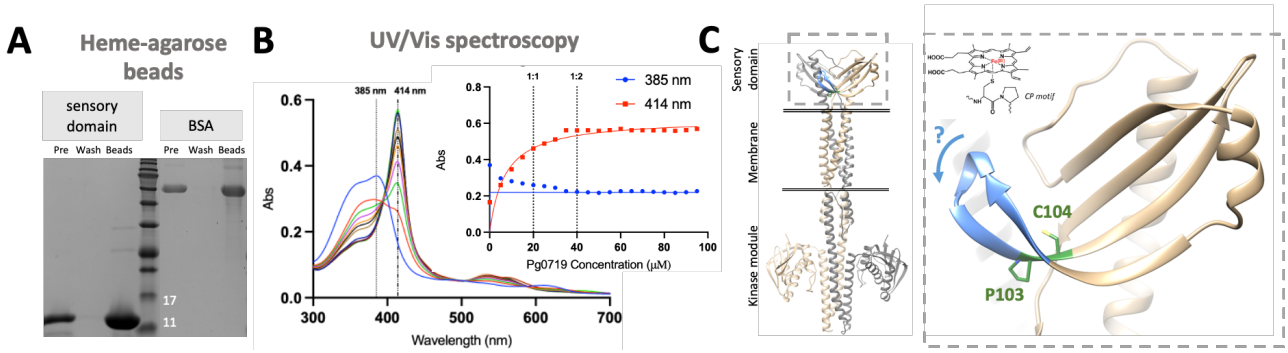

Fig 5. PG0719 heme binding – preliminary results and working model. (A) PG0719 sensory domain can irreversibly bind to heme-coated agarose beads. Bovine serum albumin (BSA) serves as a positive control. (B) Absorption spectra of PG0719 sensory domain titrated into heme. The absorbance at 415 nm represents the protein-bound heme reaching saturation with a Km of ~15 mM, while the absorbance at 385 nm represents the free-heme. (C) Left- AlphaFold predicted model of dimeric PG0719. Right - The highlighted dashed box is a zoom view of a monomeric sensory domain with the conserved PC motif highlighted in green while the b-hairpin, predicted to undergo conformational changes upon heme or its degradation products binding, in blue. The typical coordination of heme to the PC motif appears in the top of the dashed box.

these parameters will allow us to establish their relative affinity to the protein. Here, we will record the absorbance shifts from the commercially available metabolites and the purified protein constructs obtained in Aim 3.1. Notably, the initial screening step in the spectroscopic binding assays requires a substantial amount of purified protein. As the production of large amounts of soluble proteins is often more sustainable than those of membrane proteins, using the soluble periplasmic sensory domain for our initial *in vitro* screening has a significant advantage. This standalone soluble sensory domain, directly involved in signal sensing, will allow the characterizing of the activation signal, independent of the full-length protein. Once specific metabolite binding is identified, it will be further validated by individual titrations with the purified full-length protein to obtain the binding parameters in the context of the entire protein. Next, we will mutate the PC pair residues and repeat these measurements to evaluate the binding of the identified metabolite at the predicted binding site. So far, our preliminary results clearly demonstrate that the standalone sensory domain can bind heme (Fig. 5B). Lastly, we will investigate the ability of these identified binders to alter the transcript levels of select target genes in the K-antigen capsule locus and genes flanking the 77bpIR element at other sites on the chromosome (PG0106, PG0108, PG0121, PG0498, PG1780, PG1174, with PG0880 as control) *in vivo* by qPCR (81). Overall, this sub-aim will elucidate the binding characteristics and constants of PG0719 with different metabolites *such as* heme, and/or its by-products, that are released upon lysis of erythrocytes*, e.g.,* porphyrin IX, biliverdin and bilirubin.

Aim 3.3 Structural determination and characterization of PG0719 in complex with its identified metabolite(s). The recent advanced in structure prediction AI-based algorithms (such as AlphaFold) allows the researchers to obtain a 3D model of a desired protein sequence (113-115). Subjecting PG0719 sequence to AI-based structure prediction resulted in a model that cannot elucidate *(a)* the observed binding of heme or its degradation products to the sensory domain, *(b)* signal relay from the periplasmic sensory domain to the cytosolic kinase domain nor *(c)* correct dimerization interface as several potential interfaces were predicted without a computational-based method to validate them. Notably, the major discrepancy from the predicted structure was observed at the sensory domain's binding site, and in particular next to the PC binding motif. Heme-binding by a PC motif often involves the perpendicular positioning of a heme molecule a planner fashion supporting the coordination of the iron center above the Cys side chain (Fig. 5C). Here, in PG0719's predicted AI-generated model, no room to accommodate our predicted metabolite(s) could be observed, especially when their typical mode of binding is being considered. Therefore, our working hypothesis is that a substantial conformational change in the sensory domain is induced upon substrate binding, particularly in residues 92-103 that form a beta-hairpin that shelters the predicted binding site in the apo-model (Fig. 5C). To unambiguously decipher the true structure, associated binding mechanism and signal rely through the PG0719 sensor histidine kinase, we aim to experimentally determine the structure of the full-length protein. Based on PG0719 monomeric full-length size (~50 KDa), predicted dimerization ability, and receptor flexibility, we use the single-particle cryo-electron microscopy (cryoEM) method (embedded within a detergent micelle or membrane-mimetics system, which also increases particle dimensions) for its structure determination. Notably, these mimetics systems have been proven to facilitate membrane protein structure determination by single-particle cryoEM. Recent advances in direct electron detector cameras and image processing algorithms have transformed cryo-electron microscopy

into a structural biology technique capable of generating high-resolution structural information of previously intractable, conformationally dynamic, and heterogeneous membrane protein assemblies. Additionally, cryo-EM has also shown great promise for the structural characterization of membrane proteins. The Zeytuni group leverages the world-class Facility for Electron Microscopy Research (FEMR) at McGill University to conduct our structural studies of PG0719. First, our purified PG0719 in a detergent or membrane-mimetic system will be screened for optimal cryo-freezing conditions on carbon grids. Then, vitrification of the samples is performed using a Vitrobot and these grids are screened using the Tecnai F20 Transition Electron Microscope (TEM). Once cryo-conditions and grid preparation have been optimized, we collect large dataset datasets comprised of 300K-400K particle images in the Titan Krios microscope. These images are then subjected to well-established image processing pipelines using Relion (116) and/or CryoSPARC (117) to obtain the high-resolution cryoEM maps of PG0719. Potential molecular motions between the components or domains of the protein complexes are characterized using multibody refinement approaches as implemented in Relion (116) If the obtained resolution of the cryoEM map is better than 4Å, we can assign the atomic model by *de novo* building methods. To this end, we use algorithms for structure prediction and model building implemented in Rosetta (118) and PHENIX (119). The final model is built in automated tools (120) manually (121) with successive rounds of real space refinement using PHENIX (119) package. Taken together, the data introduces sufficient constraints for an unambiguous assignment of the densities in the cryoEM map.

To obtain structural and functional information of PG0719, the different conformers, transition states and metabolite-bound states, mutants with altered phosphorylation abilities (such as the catalytic histidine) are studied. In addition, we use ATP/ADP or their stable analogs along with hemin, or other identified metabolites, to explore conformational states representing different signaling stages.

Next, our experientially determined atomic models are used to explore the binding interface(s) between PG0719 and the identified metabolite or activation signal. We will then use mutational studies to further characterize key residues involved in binding, similar to as described in Aim 3.2. If a metabolite or activation signal molecule is found not to be bound to the sensory domain in our reconstructed map, we will use the structural information of the binding pocket to learn about the chemical and structural characteristics of the potential molecule(s) bound. We will use molecular docking *in silico* to model this potential interaction and further validate it via mutational studies *in vitro* and *in vivo*, as described in aim 3.2. Overall, we will determine the atomic structure of PG0719 in different signaling stages and in complex with its activating metabolite.

Aim 3 Outcomes/alternatives: The proposed aim will elucidate the activation signal(s) or metabolite(s) for the PG0719-PG0720 TCS and allow us to better understand its exact role in the Pg's response to altering oral environments. We will provide novel structural and functional insights associated with the molecular mechanism of this signal transduction cascade. These, in turn, will allow us to identify key residues and interfaces associated with ligand sensing and downstream function. In the event of challenges in functional protein production in *E. coli*, we will recombinantly overexpress and purify PG0719 in Pg, as described (122-124). Furthermore, as membrane protein's function can alter in detergent micelles, we will explore incorporating our purified PG0719 into membrane-mimetics or detergent-free systems, supporting its function in a native-like environment, and evaluate its function accordingly -these systems, including nanodiscs (125), Peptidisc (126), amphipols (127), and styrene-maleic acid polymers (SMALPs) (128). Although our preliminary studies strongly support our working hypothesis that heme is a ligand for PG0719, if this does not prove to be true, we will screen the purified sensory domain of PG0719 against commercial small-molecule and compound libraries, available through McGill's High-throughput Screening Facility to decipher the system's activation signal. Lastly, in case of challenges determining the full-length structure using cryoEM, we will use X-ray crystallography to determine the structure of PG0719's sensory domain (~13 KDa) or the cytosolic kinase module (~30 KDa).

Rigor/ Reproducibility and Statistical Analysis. All genetic constructs will be verified by sequencing and at least four clones will be generated and validated for each *P. gingivalis* deletion mutant. We will continue to conduct a rigorous cultivation protocol that pays close attention to the microbial environment during growth of *P. gingivalis*. We do not routinely passage strains. Work and all datasets will be made available in public repositories. All data sets that require statistical analysis will be robust with 3-5 biologic replicates, and inter-assay technical replicates where appropriate. For all experiments, data will be imported into PRISM statistical analysis software (GraphPad), tested for normal distribution (Shapiro-Wilk test), and both descriptive and comparative analyses will be performed. T-tests and ANOVA with parametric or non-parametric *post-hoc* testing will be performed, and data will be presented as means ± standard error. Differences in the data will be considered significant when the probability value is <5.0% (P-value < 0.05).

Timeline: All three aims are interconnected and will be on-going for 5 years.

References cited

1. Byrne SJ, Dashper SG, Darby IB, Adams GG, Hoffmann B, Reynolds EC. Progression of chronic periodontitis can be predicted by the levels of *Porphyromonas gingivalis* and *Treponema denticola* in subgingival plaque. Oral microbiology and immunology. 2009;24(6):469-77. doi: 10.1111/j.1399-302X.2009.00544.x. PubMed PMID: 19832799.
2. Darveau RP. Periodontitis: a polymicrobial disruption of host homeostasis. Nature reviews Microbiology. 2010;8(7):481-90. Epub 2010/06/02. doi: 10.1038/nrmicro2337. PubMed PMID: 20514045.
3. Lamont RJ, Jenkinson HF. Life below the gum line: pathogenic mechanisms of *Porphyromonas gingivalis*. Microbiology and Molecular Biology Reviews. 1998;62(4):1244-63. doi: 10.1128/MMBR.62.4.1244-1263.1998. PubMed PMID: 9841671; PMCID: PMC98945.
4. Socransky SS, Haffajee AD, Cugini MA, Smith C, Kent RL, Jr. Microbial complexes in subgingival plaque. Journal of Clinical Periodontology. 1998;25(2):134-44. Epub 1998/03/12. PubMed PMID: 9495612.
5. Brunner J, Scheres N, El Idrissi NB, Deng DM, Laine ML, van Winkelhoff AJ, Crielaard W. The capsule of *Porphyromonas gingivalis* reduces the immune response of human gingival fibroblasts. BMC microbiology. 2010;10:5. Epub 2010/01/13. doi: 10.1186/1471-2180-10-5. PubMed PMID: 20064245; PMCID: 2817674.
6. Whitfield C. Biosynthesis and assembly of capsular polysaccharides in Escherichia coli. Annu Rev Biochem. 2006;75:39-68. Epub 2006/06/08. doi: 10.1146/annurev.biochem.75.103004.142545. PubMed PMID: 16756484.
7. Cress BF, Englaender JA, He W, Kasper D, Linhardt RJ, Koffas MA. Masquerading microbial pathogens: capsular polysaccharides mimic host-tissue molecules. FEMS microbiology reviews. 2014;38(4):660-97. doi: 10.1111/1574-6976.12056. PubMed PMID: 24372337; PMCID: 4120193.
8. Singh A, Wyant T, Anaya-Bergman C, Aduse-Opoku J, Brunner J, Laine ML, Curtis MA, Lewis JP. The capsule of *Porphyromonas gingivalis* leads to a reduction in the host inflammatory response, evasion of phagocytosis, and increase in virulence. Infection and immunity. 2011;79(11):4533-42. Epub 2011/09/14. doi: IAI.05016-11 [pii]
10.1128/IAI.05016-11. PubMed PMID: 21911459; PMCID: 3257911.
9. Laine ML, van Winkelhoff AJ. Virulence of six capsular serotypes of *Porphyromonas gingivalis* in a mouse model. Oral microbiology and immunology. 1998;13(5):322-5.
10. Irshad M, van der Reijden WA, Crielaard W, Laine ML. In Vitro Invasion and Survival of *Porphyromonas gingivalis* in Gingival Fibroblasts; Role of the Capsule. Archivum immunologiae et therapiae experimentalis. 2012. Epub 2012/09/06. doi: 10.1007/s00005-012-0196-8. PubMed PMID: 22949096.
11. Diaz-Zuniga J, More J, Melgar-Rodriguez S, Jimenez-Union M, Villalobos-Orchard F, Munoz-Manriquez C, Monasterio G, Valdes JL, Vernal R, Paula-Lima A. Alzheimer's Disease-Like Pathology Triggered by *Porphyromonas gingivalis* in Wild Type Rats Is Serotype Dependent. Front Immunol. 2020;11:588036. Epub 2020/11/27. doi: 10.3389/fimmu.2020.588036. PubMed PMID: 33240277; PMCID: PMC7680957.
12. Nelson KE, Fleischmann RD, DeBoy RT, Paulsen IT, Fouts DE, Eisen JA, Daugherty SC, Dodson RJ, Durkin AS, Gwinn M, Haft DH, Kolonay JF, Nelson WC, Mason T, Tallon L, Gray J, Granger D, Tettelin H, Dong H, Galvin JL, Duncan MJ, Dewhirst FE, Fraser CM. Complete genome sequence of the oral pathogenic bacterium *Porphyromonas gingivalis* strain W83. Journal of bacteriology. 2003;185(18):5591-601. Epub 2003/09/02. PubMed PMID: 12949112; PMCID: 193775.
13. Aduse-Opoku J, Slaney JM, Hashim A, Gallagher A, Gallagher RP, Rangarajan M, Boutaga K, Laine ML, Van Winkelhoff AJ, Curtis MA. Identification and characterization of the capsular polysaccharide (K-antigen) locus of *Porphyromonas gingivalis*. Infect Immun. 2006;74(1):449-60.

14. Davey ME, Duncan MJ. Enhanced biofilm formation and loss of capsule synthesis: deletion of a putative glycosyltransferase in *Porphyromonas gingivalis*. Journal of bacteriology. 2006;188(15):5510-23. doi: 10.1128/JB.01685-05. PubMed PMID: 16855241; PMCID: PMC1540017.
15. Nakao R, Senpuku H, Watanabe H. *Porphyromonas gingivalis* galE is involved in lipopolysaccharide O-antigen synthesis and biofilm formation. Infection and immunity. 2006;74(11):6145-53. PubMed PMID: 16954395.
16. Alberti-Segui C, Arndt A, Cugini C, Priyadarshini R, Davey ME. HU protein affects transcription of surface polysaccharide synthesis genes in *Porphyromonas gingivalis*. Journal of bacteriology. 2010;192(23):6217-29. Epub 2010/10/05. doi: 10.1128/JB.00106-10. PubMed PMID: 20889748; PMCID: 2981211.
17. Priyadarshini R, Cugini C, Arndt A, Chen T, Tjokro NO, Goodman SD, Davey ME. The nucleoid-associated protein HUbeta affects global gene expression in *Porphyromonas gingivalis*. Microbiology. 2013;159(Pt 2):219-29. doi: 10.1099/mic.0.061002-0. PubMed PMID: 23175503; PMCID: 3709559.
18. Shoji M, Sato K, Yukitake H, Naito M, Nakayama K. Involvement of the Wbp pathway in the biosynthesis of *Porphyromonas gingivalis* lipopolysaccharide with anionic polysaccharide. Scientific reports. 2014;4:5056. doi: 10.1038/srep05056. PubMed PMID: 24852504; PMCID: 4031482.
19. Slaney JM, Curtis MA. Mechanisms of evasion of complement by *Porphyromonas gingivalis*. Front Biosci. 2008;13:188-96. PubMed PMID: 17981537.
20. Maeda K, Tribble GD, Tucker CM, Anaya C, Shizukuishi S, Lewis JP, Demuth DR, Lamont RJ. A *Porphyromonas gingivalis* tyrosine phosphatase is a multifunctional regulator of virulence attributes. Molecular Microbiology. 2008;69(5):1153-64. PubMed PMID: 18573179.
21. Simionato MR, Tucker CM, Kuboniwa M, Lamont G, Demuth DR, Tribble GD, Lamont RJ. *Porphyromonas gingivalis* genes involved in community development with *Streptococcus gordonii*. Infection and immunity. 2006;74(11):6419-28. Epub 2006/08/23. doi: 10.1128/IAI.00639-06. PubMed PMID: 16923784; PMCID: 1695522.
22. Wright CJ, Xue P, Hirano T, Liu C, Whitmore SE, Hackett M, Lamont RJ. Characterization of a bacterial tyrosine kinase in *Porphyromonas gingivalis* involved in polymicrobial synergy. MicrobiologyOpen. 2014;3(3):383-94. doi: 10.1002/mbo3.177. PubMed PMID: 24811194.
23. Kim H-M, Ranjit DK, Walker AR, Getachew H, Progulske-Fox A, Davey ME. A Novel Regulation of K-antigen Capsule Synthesis in *Porphyromonas gingivalis* Is Driven by the Response Regulator PG0720-Directed Antisense RNA. Frontiers in Oral Health. 2021;2(41). doi: 10.3389/froh.2021.701659.
24. Rouviere-Yaniv J, Gros F. Characterization of a novel, low-molecular-weight DNA-binding protein from Escherichia coli. Proceedings of the National Academy of Sciences of the United States of America. 1975;72(9):3428-32. PubMed PMID: 1103148.
25. Fernandez S, Rojo F, Alonso JC. The Bacillus subtilis chromatin-associated protein Hbsu is involved in DNA repair and recombination. Molecular Microbiology. 1997;23(6):1169-79. PubMed PMID: 9106208.
26. Kohler P, Marahiel MA. Mutational analysis of the nucleoid-associated protein HBsu of Bacillus subtilis. Mol Gen Genet. 1998;260(5):487-91. PubMed PMID: 9894920.
27. Swinger KK, Rice PA. IHF and HU: flexible architects of bent DNA. Current opinion in structural biology. 2004;14(1):28-35. PubMed PMID: 15102446.
28. Sheridan SD, Benham CJ, Hatfield GW. Activation of gene expression by a novel DNA structural transmission mechanism that requires supercoiling-induced DNA duplex destabilization in an upstream activating sequence. The Journal of biological chemistry. 1998;273(33):21298-308. PubMed PMID: 9694890.
29. Boubrik F, Rouviere-Yaniv J. Increased sensitivity to gamma irradiation in bacteria lacking protein HU. Proceedings of the National Academy of Sciences of the United States of America. 1995;92(9):3958-62. PubMed PMID: 7732012.

30. Dri AM, Rouviere-Yaniv J, Moreau PL. Inhibition of cell division in *hupA hupB* mutant bacteria lacking HU protein. Journal of bacteriology. 1991;173(9):2852-63. PubMed PMID: 2019558.
31. Giangrossi M, Giuliodori AM, Gualerzi CO, Pon CL. Selective expression of the beta-subunit of nucleoid-associated protein HU during cold shock in Escherichia coli. Molecular Microbiology. 2002;44(1):205-16. PubMed PMID: 11967080.
32. Li S, Waters R. Escherichia coli strains lacking protein HU are UV sensitive due to a role for HU in homologous recombination. Journal of bacteriology. 1998;180(15):3750-6. PubMed PMID: 9683467.
33. Miyabe I, Zhang QM, Kano Y, Yonei S. Histone-like protein HU is required for recA gene-dependent DNA repair and SOS induction pathways in UV-irradiated *Escherichia coli*. International journal of radiation biology. 2000;76(1):43-9. PubMed PMID: 10665956.
34. Friedman DI. Integration host factor: a protein for all reasons. Cell. 1988;55(4):545-54. Epub 1988/11/18. PubMed PMID: 2972385.
35. Morales P, Rouviere-Yaniv J, Dreyfus M. The histone-like protein HU does not obstruct movement of T7 RNA polymerase in *Escherichia coli* cells but stimulates its activity. Journal of bacteriology. 2002;184(6):1565-70. PubMed PMID: 11872707.
36. Balandina A, Claret L, Hengge-Aronis R, Rouviere-Yaniv J. The *Escherichia coli* histone-like protein HU regulates rpoS translation. Molecular Microbiology. 2001;39(4):1069-79. PubMed PMID: 11251825.
37. Balandina A, Kamashev D, Rouviere-Yaniv J. The bacterial histone-like protein HU specifically recognizes similar structures in all nucleic acids. DNA, RNA, and their hybrids. The Journal of biological chemistry. 2002;277(31):27622-8. PubMed PMID: 12006568.
38. Jacob-Dubuisson F, Mechaly A, Betton JM, Antoine R. Structural insights into the signalling mechanisms of two-component systems. Nature Reviews Microbiology. 2018;16(10):585-93. doi: 10.1038/s41579-018-0055-7. PubMed PMID: WOS:000444578100006.
39. Scott JC, Klein BA, Duran-Pinedo A, Hu LD, Duncan MJ. A Two-Component System Regulates Hemin Acquisition in *Porphyromonas gingivalis*. Plos One. 2013;8(9). doi: ARTN e73351 10.1371/journal.pone.0073351. PubMed PMID: WOS:000324481600066.
40. Gottesman S, Storz G. Bacterial small RNA regulators: versatile roles and rapidly evolving variations. Cold Spring Harbor perspectives in biology. 2011;3(12). Epub 2011/12/01. doi: 10.1101/cshperspect.a003798. PubMed PMID: 20980440; PMCID: PMC3225950.
41. Repoila F, Majdalani N, Gottesman S. Small non-coding RNAs, co-ordinators of adaptation processes in *Escherichia coli*: the RpoS paradigm. Molecular Microbiology. 2003;48(4):855-61. PubMed PMID: 12753181.
42. Altuvia S. Identification of bacterial small non-coding RNAs: experimental approaches. Current opinion in microbiology. 2007;10(3):257-61. doi: 10.1016/j.mib.2007.05.003. PubMed PMID: 17553733.
43. Arnedo J, Romero-Zaliz R, Zwir I, Del Val C. A multiobjective method for robust identification of bacterial small non-coding RNAs. Bioinformatics. 2014;30(20):2875-82. doi: 10.1093/bioinformatics/btu398. PubMed PMID: 24958812.
44. Brantl S, Bruckner R. Small regulatory RNAs from low-GC Gram-positive bacteria. RNA biology. 2014;11(5):443-56. doi: 10.4161/rna.28036. PubMed PMID: 24576839.
45. Gottesman S. Micros for microbes: non-coding regulatory RNAs in bacteria. Trends in genetics : TIG. 2005;21(7):399-404. doi: 10.1016/j.tig.2005.05.008. PubMed PMID: 15913835.
46. Mraheil MA, Billion A, Kuenne C, Pischimarov J, Kreikemeyer B, Engelmann S, Hartke A, Giard JC, Rupnik M, Vorwerk S, Beier M, Retey J, Hartsch T, Jacob A, Cemic F, Hemberger J, Chakraborty T, Hain T. Comparative genome-wide analysis of small RNAs of major Gram-positive pathogens: from identification to application. Microbial biotechnology. 2010;3(6):658-76. doi: 10.1111/j.1751-7915.2010.00171.x. PubMed PMID: 21255362; PMCID: 3815340.

47. Repoila F, Darfeuille F. Small regulatory non-coding RNAs in bacteria: physiology and mechanistic aspects. Biology of the cell / under the auspices of the European Cell Biology Organization. 2009;101(2):117-31. doi: 10.1042/BC20070137. PubMed PMID: 19076068.
48. Sharma CM, Vogel J. Experimental approaches for the discovery and characterization of regulatory small RNA. Current opinion in microbiology. 2009;12(5):536-46. doi: 10.1016/j.mib.2009.07.006. PubMed PMID: 19758836.
49. Storz G, Vogel J, Wassarman KM. Regulation by small RNAs in bacteria: expanding frontiers. Mol Cell. 2011;43(6):880-91. doi: 10.1016/j.molcel.2011.08.022. PubMed PMID: 21925377; PMCID: 3176440.
50. Vogel J, Wagner EG. Target identification of small noncoding RNAs in bacteria. Current opinion in microbiology. 2007;10(3):262-70. doi: 10.1016/j.mib.2007.06.001. PubMed PMID: 17574901.
51. Waters LS, Storz G. Regulatory RNAs in bacteria. Cell. 2009;136(4):615-28. doi: 10.1016/j.cell.2009.01.043. PubMed PMID: 19239884; PMCID: 3132550.
52. Romeo T, Vakulskas CA, Babitzke P. Post-transcriptional regulation on a global scale: form and function of Csr/Rsm systems. Environmental microbiology. 2013;15(2):313-24. doi: 10.1111/j.1462-2920.2012.02794.x. PubMed PMID: 22672726; PMCID: 3443267.
53. Michaux C, Verneuil N, Hartke A, Giard JC. Physiological roles of small RNA molecules. Microbiology. 2014;160(Pt 6):1007-19. doi: 10.1099/mic.0.076208-0. PubMed PMID: 24694375.
54. Wagner EG. Cycling of RNAs on Hfq. RNA biology. 2013;10(4):619-26. doi: 10.4161/rna.24044. PubMed PMID: 23466677; PMCID: 3710369.
55. Macvanin M, Edgar R, Cui F, Trostel A, Zhurkin V, Adhya S. Noncoding RNAs binding to the nucleoid protein HU in *Escherichia coli*. Journal of bacteriology. 2012;194(22):6046-55. doi: 10.1128/JB.00961-12. PubMed PMID: 22942248; PMCID: 3486375.
56. Georg J, Hess WR. cis-antisense RNA, another level of gene regulation in bacteria. Microbiology and Molecular Biology Reviews. 2011;75(2):286-300. doi: 10.1128/MMBR.00032-10. PubMed PMID: 21646430; PMCID: 3122628.
57. Thomason MK, Storz G. Bacterial antisense RNAs: how many are there, and what are they doing? Annual review of genetics. 2010;44:167-88. doi: 10.1146/annurev-genet-102209-163523. PubMed PMID: 20707673; PMCID: PMC3030471.
58. Nicolson GL. The Fluid-Mosaic Model of Membrane Structure: still relevant to understanding the structure, function and dynamics of biological membranes after more than 40 years. Biochimica et biophysica acta. 2014;1838(6):1451-66. Epub 2013/11/01. doi: 10.1016/j.bbamem.2013.10.019. PubMed PMID: 24189436.
59. Hannun YA, Obeid LM. Principles of bioactive lipid signalling: lessons from sphingolipids. Nature reviews. 2008;9(2):139-50. doi: 10.1038/nrm2329. PubMed PMID: 18216770.
60. Futerman AH, Riezman H. The ins and outs of sphingolipid synthesis. Trends Cell Biol. 2005;15(6):312-8. Epub 2005/06/15. doi: 10.1016/j.tcb.2005.04.006. PubMed PMID: 15953549.
61. Olsen I, Nichols FC. Are Sphingolipids and Serine Dipeptide Lipids Underestimated Virulence Factors of *Porphyromonas gingivalis*? Infection and immunity. 2018;86(7). Epub 2018/04/11. doi: 10.1128/IAI.00035-18. PubMed PMID: 29632248; PMCID: PMC6013676.
62. Nichols FC, Yao X, Bajrami B, Downes J, Finegold SM, Knee E, Gallagher JJ, Housley WJ, Clark RB. Phosphorylated dihydroceramides from common human bacteria are recovered in human tissues. PLoS One. 2011;6(2):e16771. Epub 2011/02/11. doi: 10.1371/journal.pone.0016771. PubMed PMID: 21347306; PMCID: PMC3037954.
63. Nichols FC, Riep B, Mun J, Morton MD, Bojarski MT, Dewhirst FE, Smith MB. Structures and biological activity of phosphorylated dihydroceramides of *Porphyromonas gingivalis*. Journal of lipid research. 2004;45(12). doi: 10.1194/jlr.M400278-JLR200. PubMed PMID: 15466368.
64. Nichols FC. Novel ceramides recovered from *Porphyromonas gingivalis*: relationship to adult periodontitis. Journal of lipid research. 1998;39(12):2360-72. PubMed PMID: 9831624.

65. An D, Na C, Bielawski J, Hannun YA, Kasper DL. Membrane sphingolipids as essential molecular signals for Bacteroides survival in the intestine2011. doi: 10.1073/pnas.1001501107.
66. Moye ZD, Valiuskyte K, Dewhirst FE, Nichols FC, Davey ME. Synthesis of Sphingolipids Impacts Survival of *Porphyromonas gingivalis* and the Presentation of Surface Polysaccharides. Front Microbiol. 2016;7:1919. Epub 2016/11/29. doi: 10.3389/fmicb.2016.01919. PubMed PMID: 27965646; PMCID: PMC5126122.
67. An D, Oh SF, Olszak T, Neves JF, Avci FY, Erturk-Hasdemir D, Lu X, Zeissig S, Blumberg RS, Kasper DL. Sphingolipids from a symbiotic microbe regulate homeostasis of host intestinal natural killer T cells. Cell. 2014;156(1-2):123-33. doi: 10.1016/j.cell.2013.11.042. PubMed PMID: 24439373; PMCID: PMC3909465.
68. Heaver SL, Johnson EL, Ley RE. Sphingolipids in host-microbial interactions. Current opinion in microbiology. 2018;43:92-9. Epub 2018/01/13. doi: 10.1016/j.mib.2017.12.011. PubMed PMID: 29328957.
69. Olea-Ozuna RJ, Poggio S, EdBergstrom, Quiroz-Rocha E, Garcia-Soriano DA, Sahonero-Canavesi DX, Padilla-Gomez J, Martinez-Aguilar L, Lopez-Lara IM, Thomas-Oates J, Geiger O. Five structural genes required for ceramide synthesis in Caulobacter and for bacterial survival. Environmental microbiology. 2021;23(1):143-59. Epub 2020/10/17. doi: 10.1111/1462-2920.15280. PubMed PMID: 33063925.
70. Stankeviciute G, Guan Z, Goldfine H, Klein EA. Caulobacter crescentus Adapts to Phosphate Starvation by Synthesizing Anionic Glycoglycerolipids and a Novel Glycosphingolipid. mBio. 2019;10(2). Epub 2019/04/04. doi: 10.1128/mBio.00107-19. PubMed PMID: 30940701; PMCID: PMC6445935.
71. Wieland Brown LC, Penaranda C, Kashyap PC, Williams BB, Clardy J, Kronenberg M, Sonnenburg JL, Comstock LE, Bluestone JA, Fischbach MA. Production of alpha-galactosylceramide by a prominent member of the human gut microbiota. PLoS Biol. 2013;11(7):e1001610. doi: 10.1371/journal.pbio.1001610. PubMed PMID: 23874157; PMCID: PMC3712910.
72. Rocha FG, Moye ZD, Ottenberg G, Tang P, Campopiano DJ, Gibson FC, 3rd, Davey ME. *Porphyromonas gingivalis* Sphingolipid Synthesis Limits the Host Inflammatory Response. Journal of Dental Research. 2020;99(5):568-76. Epub 2020/02/28. doi: 10.1177/0022034520908784. PubMed PMID: 32105543; PMCID: PMC7174802.
73. Rocha FG, Moye ZD, Ottenberg G, Tang P, Campopiano DJ, Gibson FC, Davey ME. Sphingolipid Synthesis Limits the Host Inflammatory Response. Journal of Dental Research. 2020;99(5):568-76. Epub 2020/02/27. doi: 10.1177/0022034520908784. PubMed PMID: 32105543; PMCID: PMC7174802.
74. Ranjit DK, Moye ZD, Rocha FG, Ottenberg G, Nichols FC, Kim HM, Walker AR, Gibson FC, 3rd, Davey ME. Characterization of a Bacterial Kinase That Phosphorylates Dihydrosphingosine to Form dhS1P. Microbiol Spectr. 2022;10(2):e0000222. Epub 2022/03/15. doi: 10.1128/spectrum.00002-22. PubMed PMID: 35286133; PMCID: PMC9045371.
75. Tjokro NO, Rocco CJ, Priyadarshini R, Davey ME, Goodman SD. A biochemical analysis of the interaction of *Porphyromonas gingivalis* HU PG0121 protein with DNA. PLoS One. 2014;9(3):e93266. doi: 10.1371/journal.pone.0093266. PubMed PMID: 24681691; PMCID: 3969353.
76. Klein BA, Tenorio EL, Lazinski DW, Camilli A, Duncan MJ, Hu LT. Identification of essential genes of the periodontal pathogen *Porphyromonas gingivalis*. BMC Genomics. 2012;13:578. doi: 10.1186/1471-2164-13-578. PubMed PMID: 23114059; PMCID: 3547785.
77. Tanaka H, Goshima N, Kohno K, Kano Y, Imamoto F. Properties of DNA-binding of HU heterotypic and homotypic dimers from *Escherichia coli*. Journal of biochemistry. 1993;113(5):568-72. Epub 1993/05/01. PubMed PMID: 8340349.
78. van Winkelhoff AJ, Appelmelk BJ, Kippuw N, de Graaff J. K-antigens in *Porphyromonas gingivalis* are associated with virulence. Oral microbiology and immunology. 1993;8(5):259-65. PubMed PMID: 8265200.

79. Bainbridge BW, Hirano T, Grieshaber N, Davey ME. Deletion of a 77-base-pair inverted repeat element alters the synthesis of surface polysaccharides in *Porphyromonas gingivalis*. Journal of bacteriology. 2015;197(7):1208-20. Epub 2015/01/26. doi: 10.1128/JB.02589-14. PubMed PMID: 25622614; PMCID: PMC4352660.
80. Scott JC, Klein BA, Duran-Pinedo A, Hu L, Duncan MJ. A two-component system regulates hemin acquisition in *Porphyromonas gingivalis*. PLoS One. 2013;8(9):e73351. doi: 10.1371/journal.pone.0073351. PubMed PMID: 24039921; PMCID: 3764172.
81. Kim HM, Davey ME. Synthesis of ppGpp impacts type IX secretion and biofilm matrix formation in *Porphyromonas gingivalis*. NPJ Biofilms Microbiomes. 2020;6(1):5. Epub 2020/02/02. doi: 10.1038/s41522-020-0115-4. PubMed PMID: 32005827; PMCID: PMC6994654.
82. Moradali MF, Ghods S, Bahre H, Lamont RJ, Scott DA, Seifert R. Atypical cyclic di-AMP signaling is essential for *Porphyromonas gingivalis* growth and regulation of cell envelope homeostasis and virulence. NPJ Biofilms Microbiomes. 2022;8(1):53. Epub 2022/07/07. doi: 10.1038/s41522-022-00316-w. PubMed PMID: 35794154; PMCID: PMC9259658.
83. Solbiati J, Duran-Pinedo A, Godoy Rocha F, Gibson FC, 3rd, Frias-Lopez J. Virulence of the Pathogen *Porphyromonas gingivalis* Is Controlled by the CRISPR-Cas Protein Cas3. mSystems. 2020;5(5). Epub 2020/10/01. doi: 10.1128/mSystems.00852-20. PubMed PMID: 32994292; PMCID: PMC7527141.
84. Jutras BL, Verma A, Stevenson B. Identification of novel DNA-binding proteins using DNA-affinity chromatography/pull down. Curr Protoc Microbiol. 2012;Chapter 1:Unit1F Epub 2012/02/07. doi: 10.1002/9780471729259.mc01f01s24. PubMed PMID: 22307548; PMCID: PMC3564586.
85. Hagmann CA, Herzner AM, Abdullah Z, Zillinger T, Jakobs C, Schuberth C, Coch C, Higgins PG, Wisplinghoff H, Barchet W, Hornung V, Hartmann G, Schlee M. RIG-I detects triphosphorylated RNA of Listeria monocytogenes during infection in non-immune cells. PLoS One. 2013;8(4):e62872. doi: 10.1371/journal.pone.0062872. PubMed PMID: 23653683; PMCID: 3639904.
86. Christopher AB, Arndt A, Cugini C, Davey ME. A streptococcal effector protein that inhibits *Porphyromonas gingivalis* biofilm development. Microbiology. 2010;156(Pt 11):3469-77. Epub 2010/08/14. doi: 10.1099/mic.0.042671-0. PubMed PMID: 20705665.
87. Cugini C, Stephens DN, Nguyen D, Kantarci A, Davey ME. Arginine deiminase inhibits *Porphyromonas gingivalis* surface attachment. Microbiology. 2013;159(Pt 2):275-85. doi: 10.1099/mic.0.062695-0. PubMed PMID: 23242802; PMCID: 3709564.
88. Davey ME, Costerton JW. Molecular genetics analyses of biofilm formation in oral isolates. Periodontology 2000. 2006;42:13-26. Epub 2006/08/26. doi: 10.1111/j.1600-0757.2006.00052.x. PubMed PMID: 16930303.
89. Bush M, Dixon R. The role of bacterial enhancer binding proteins as specialized activators of sigma54-dependent transcription. Microbiology and Molecular Biology Reviews. 2012;76(3):497-529. doi: 10.1128/MMBR.00006-12. PubMed PMID: 22933558; PMCID: 3429621.
90. Shingler V. Signal sensory systems that impact sigma(5)(4) -dependent transcription. FEMS microbiology reviews. 2011;35(3):425-40. doi: 10.1111/j.1574-6976.2010.00255.x. PubMed PMID: 21054445.
91. Kundukad B, Cong P, van der Maarel JR, Doyle PS. Time-dependent bending rigidity and helical twist of DNA by rearrangement of bound HU protein. Nucleic Acids Res. 2013;41(17):8280-8. Epub 2013/07/06. doi: 10.1093/nar/gkt593. PubMed PMID: 23828037; PMCID: PMC3783175.
92. Claret L, Rouviere-Yaniv J. Variation in HU composition during growth of *Escherichia coli*: the heterodimer is required for long term survival. Journal of molecular biology. 1997;273(1):93-104. PubMed PMID: 9367749.
93. Trautmann HS, Ramsey KM. A Ribosomal Protein Homolog Governs Gene Expression and Virulence in a Bacterial Pathogen. Journal of bacteriology. 2022;204(10):e0026822. Epub 2022/09/20. doi: 10.1128/jb.00268-22. PubMed PMID: 36121290; PMCID: PMC9578407.

94. Nishikawa K, Yoshimura F, Duncan MJ. A regulation cascade controls expression of *Porphyromonas gingivalis* fimbriae via the FimR response regulator. Molecular Microbiology. 2004;54(2):546-60. Epub 2004/10/08. doi: 10.1111/j.1365-2958.2004.04291.x. PubMed PMID: 15469523.
95. Finn MB, Ramsey KM, Dove SL, Wessels MR. Identification of Group A Streptococcus Genes Directly Regulated by CsrRS and Novel Intermediate Regulators. mBio. 2021;12(4):e0164221. Epub 2021/07/14. doi: 10.1128/mBio.01642-21. PubMed PMID: 34253064; PMCID: PMC8406183.
96. Kambara TK, Ramsey KM, Dove SL. Pervasive Targeting of Nascent Transcripts by Hfq. Cell Rep. 2018;23(5):1543-52. Epub 2018/05/03. doi: 10.1016/j.celrep.2018.03.134. PubMed PMID: 29719264; PMCID: PMC5990048.
97. Ramsey KM, Osborne ML, Vvedenskaya IO, Su C, Nickels BE, Dove SL. Ubiquitous promoter-localization of essential virulence regulators in Francisella tularensis. PLoS pathogens. 2015;11(4):e1004793. Epub 2015/04/02. doi: 10.1371/journal.ppat.1004793. PubMed PMID: 25830507; PMCID: PMC4382096.
98. Prieto AI, Kahramanoglou C, Ali RM, Fraser GM, Seshasayee AS, Luscombe NM. Genomic analysis of DNA binding and gene regulation by homologous nucleoid-associated proteins IHF and HU in *Escherichia coli* K12. Nucleic Acids Res. 2012;40(8):3524-37. Epub 2011/12/20. doi: 10.1093/nar/gkr1236. PubMed PMID: 22180530; PMCID: PMC3333857.
99. Ali Azam T, Iwata A, Nishimura A, Ueda S, Ishihama A. Growth phase-dependent variation in protein composition of the *Escherichia coli* nucleoid. Journal of bacteriology. 1999;181(20):6361-70. Epub 1999/10/09. PubMed PMID: 10515926; PMCID: 103771.
100. Reyes L, Eiler-McManis E, Rodrigues PH, Chadda AS, Wallet SM, Belanger M, Barrett AG, Alvarez S, Akin D, Dunn WA, Progulske-Fox A. Deletion of Lipoprotein PG0717 in *Porphyromonas gingivalis* W83 Reduces Gingipain Activity and Alters Trafficking in and Response by Host Cells. Plos One. 2013;8(9). doi: ARTN e74230
10.1371/journal.pone.0074230. PubMed PMID: WOS:000326240100092.
101. Dashper SG, Cross KJ, Slakeski N, Lissel P, Aulakh P, Moore C, Reynolds EC. Hemoglobin hydrolysis and heme acquisition by *Porphyromonas gingivalis*. Oral microbiology and immunology. 2004;19(1):50-6. PubMed PMID: 14678474.
102. O'Brien Simpson N, Veith PD, Dashper SG, Reynolds EC. *Porphyromonas gingivalis* gingipains: the molecular teeth of a microbial vampire. Current protein & peptide science. 2003;4(6):409-26. Epub 2003/12/20. PubMed PMID: 14683427.
103. Olczak T, Simpson W, Liu X, Genco CA. Iron and heme utilization in *Porphyromonas gingivalis*. FEMS microbiology reviews. 2005;29(1):119-44. Epub 2005/01/18. doi: 10.1016/j.femsre.2004.09.001. PubMed PMID: 15652979.
104. Olczak T, Sosicka P, Olczak M. HmuY is an important virulence factor for *Porphyromonas gingivalis* growth in the heme-limited host environment and infection of macrophages. Biochemical and biophysical research communications. 2015;467(4):748-53. Epub 2015/10/19. doi: 10.1016/j.bbrc.2015.10.070. PubMed PMID: 26482851.
105. Paramaesvaran M, Nguyen KA, Caldon E, McDonald JA, Najdi S, Gonzaga G, Langley DB, DeCarlo A, Crossley MJ, Hunter N, Collyer CA. Porphyrin-mediated cell surface heme capture from hemoglobin by *Porphyromonas gingivalis*. Journal of bacteriology. 2003;185(8):2528-37.
106. Simpson W, Olczak T, Genco CA. Lysine-specific gingipain K and heme/hemoglobin receptor HmuR are involved in heme utilization in *Porphyromonas gingivalis*. Acta Biochim Pol. 2004;51(1):253-62. Epub 2004/04/20. doi: 045101253. PubMed PMID: 15094847.
107. Slakeski N, Dashper SG, Cook P, Poon C, Moore C, Reynolds EC. A *Porphyromonas gingivalis* genetic locus encoding a heme transport system. Oral microbiology and immunology. 2000;15(6):388-92. Epub 2001/01/12. doi: omi150609 [pii]. PubMed PMID: 11154437.
108. Veith PD, Luong C, Tan KH, Dashper SG, Reynolds EC. Outer Membrane Vesicle Proteome of *Porphyromonas gingivalis* Is Differentially Modulated Relative to the Outer Membrane in Response to

Heme Availability. J Proteome Res. 2018;17(7):2377-89. Epub 2018/05/29. doi: 10.1021/acs.jproteome.8b00153. PubMed PMID: 29766714.
109. Kinoshita-Kikuta E, Kinoshita E, Eguchi Y, Koike T. Validation of Cis and Trans Modes in Multistep Phosphotransfer Signaling of Bacterial Tripartite Sensor Kinases by Using Phos-Tag SDS-PAGE. Plos One. 2016;11(2). doi: ARTN e0148294
10.1371/journal.pone.0148294. PubMed PMID: WOS:000369548200094.
110. Shimizu T, Lengalova A, Martinek V, Martinkova M. Heme: emergent roles of heme in signal transduction, functional regulation and as catalytic centres. Chem Soc Rev. 2019;48(24):5624-57. Epub 2019/11/22. doi: 10.1039/c9cs00268e. PubMed PMID: 31748766.
111. Chen T, Hosogi Y, Nishikawa K, Abbey K, Fleischmann RD, Walling J, Duncan MJ. Comparative whole-genome analysis of virulent and avirulent strains of *Porphyromonas gingivalis*. Journal of bacteriology. 2004;186(16):5473-9.
112. Comer JM, Zhang L. Experimental Methods for Studying Cellular Heme Signaling. Cells. 2018;7(6). Epub 2018/05/26. doi: 10.3390/cells7060047. PubMed PMID: 29795036; PMCID: PMC6025097.
113. Jumper J, Evans R, Pritzel A, Green T, Figurnov M, Ronneberger O, Tunyasuvunakool K, Bates R, Zidek A, Potapenko A, Bridgland A, Meyer C, Kohl SAA, Ballard AJ, Cowie A, Romera-Paredes B, Nikolov S, Jain R, Adler J, Back T, Petersen S, Reiman D, Clancy E, Zielinski M, Steinegger M, Pacholska M, Berghammer T, Bodenstein S, Silver D, Vinyals O, Senior AW, Kavukcuoglu K, Kohli P, Hassabis D. Highly accurate protein structure prediction with AlphaFold. Nature. 2021;596(7873):583-9. Epub 2021/07/16. doi: 10.1038/s41586-021-03819-2. PubMed PMID: 34265844; PMCID: PMC8371605 have filed non-provisional patent applications 16/701,070 and PCT/EP2020/084238, and provisional patent applications 63/107,362, 63/118,917, 63/118,918, 63/118,921 and 63/118,919, each in the name of DeepMind Technologies Limited, each pending, relating to machine learning for predicting protein structures. The other authors declare no competing interests.
114. Baek M, DiMaio F, Anishchenko I, Dauparas J, Ovchinnikov S, Lee GR, Wang J, Cong Q, Kinch LN, Schaeffer RD, Millan C, Park H, Adams C, Glassman CR, DeGiovanni A, Pereira JH, Rodrigues AV, van Dijk AA, Ebrecht AC, Opperman DJ, Sagmeister T, Buhlheller C, Pavkov-Keller T, Rathinaswamy MK, Dalwadi U, Yip CK, Burke JE, Garcia KC, Grishin NV, Adams PD, Read RJ, Baker D. Accurate prediction of protein structures and interactions using a three-track neural network. Science. 2021;373(6557):871-6. Epub 2021/07/21. doi: 10.1126/science.abj8754. PubMed PMID: 34282049; PMCID: PMC7612213.
115. Chakravarty D, Porter LL. AlphaFold2 fails to predict protein fold switching. Protein Sci. 2022;31(6):e4353. Epub 2022/06/01. doi: 10.1002/pro.4353. PubMed PMID: 35634782; PMCID: PMC9134877.
116. Zivanov J, Nakane T, Forsberg BO, Kimanius D, Hagen WJH, Lindahl E, Scheres SHW. New tools for automated high-resolution cryo-EM structure determination in RELION-3. Elife. 2018;7. doi: ARTN e42166
10.7554/eLife.42166. PubMed PMID: WOS:000450857100001.
117. Punjani A, Rubinstein JL, Fleet DJ, Brubaker MA. cryoSPARC: algorithms for rapid unsupervised cryo-EM structure determination. Nature methods. 2017;14(3):290-+. doi: 10.1038/Nmeth.4169. PubMed PMID: WOS:000395661700027.
118. Song YF, DiMaio F, Wang RYR, Kim D, Miles C, Brunette TJ, Thompson J, Baker D. High-Resolution Comparative Modeling with RosettaCM. Structure. 2013;21(10):1735-42. doi: 10.1016/j.str.2013.08.005. PubMed PMID: WOS:000326413500005.
119. Liebschner D, Afonine PV, Baker ML, Bunkoczi G, Chen VB, Croll TI, Hintze B, Hung LW, Jain S, McCoy AJ, Moriarty NW, Oeffner RD, Poon BK, Prisant MG, Read RJ, Richardson JS, Richardson DC, Sammito MD, Sobolev OV, Stockwell DH, Terwilliger TC, Urzhumtsev AG, Videau LL, Williams CJ, Adams PD. Macromolecular structure determination using X-rays, neutrons and electrons: recent developments in Phenix. Acta Crystallogr D. 2019;75:861-77. doi: 10.1107/S2059798319011471. PubMed PMID: WOS:000497657100001.

120. Perrakis A, Morris R, Lamzin V. ARP/wARP: Procedures for automated model building and refinement. Acta Crystallogr A. 2000;56:S28-S. doi: 10.1107/S010876730002153x. PubMed PMID: WOS:000475816100039.
121. Winn MD, Ballard CC, Cowtan KD, Dodson EJ, Emsley P, Evans PR, Keegan RM, Krissinel EB, Leslie AGW, McCoy A, McNicholas SJ, Murshudov GN, Pannu NS, Potterton EA, Powell HR, Read RJ, Vagin A, Wilson KS. Overview of the CCP4 suite and current developments. Acta Crystallogr D. 2011;67:235-42. doi: 10.1107/S0907444910045749. PubMed PMID: WOS:000288532800002.
122. Bereta G, Goulas T, Madej M, Bielecka E, Sola M, Potempa J, Xavier Gomis-Ruth F. Structure, function, and inhibition of a genomic/clinical variant of *Porphyromonas gingivalis* peptidylarginine deiminase. Protein Sci. 2019;28(3):478-86. Epub 2019/01/15. doi: 10.1002/pro.3571. PubMed PMID: 30638292; PMCID: PMC6371208.
123. Goulas T, Mizgalska D, Garcia-Ferrer I, Kantyka T, Guevara T, Szmigielski B, Sroka A, Millán C, Usón I, Veillard F, Potempa B, Mydel P, Solà M, Potempa J, Gomis-Rüth FX. Structure and mechanism of a bacterial host-protein citrullinating virulence factor, *Porphyromonas gingivalis* peptidylarginine deiminase. Scientific reports. 2015;5:11969. doi: 10.1038/srep11969. PubMed PMID: 26132828; PMCID: PMC4487231.
124. Veillard F, Potempa B, Guo Y, Ksiazek M, Sztukowska MN, Houston JA, Koneru L, Nguyen KA, Potempa J. Purification and characterisation of recombinant His-tagged RgpB gingipain from Porphymonas gingivalis. Biological chemistry. 2015;396(4):377-84. Epub 2015/02/27. doi: 10.1515/hsz-2014-0304. PubMed PMID: 25720118; PMCID: PMC4682895.
125. Denisov IG, Sligar SG. Nanodiscs for structural and functional studies of membrane proteins. Nature Structural & Molecular Biology. 2016;23(6):481-6. doi: 10.1038/nsmb.3195. PubMed PMID: WOS:000377421800005.
126. Carlson ML, Young JW, Zhao ZY, Fabre L, Jun D, Li JN, Li J, Dhupar HS, Wason I, Mills AT, Beatty JT, Klassen JS, Rouiller I, Duong F. The Peptidisc, a simple method for stabilizing membrane proteins in detergent-free solution. Elife. 2018;7. doi: ARTN e34085
10.7554/eLife.34085. PubMed PMID: WOS:000441499900001.
127. Tribet C, Audebert R, Popot JL. Amphipols: Polymers that keep membrane proteins soluble in aqueous solutions. Proceedings of the National Academy of Sciences of the United States of America. 1996;93(26):15047-50. doi: DOI 10.1073/pnas.93.26.15047. PubMed PMID: WOS:A1996WC20400012.
128. Postis V, Rawson S, Mitchell JK, Lee SC, Parslow RA, Dafforn TR, Baldwin SA, Muench SP. The use of SMALPs as a novel membrane protein scaffold for structure study by negative stain electron microscopy. Bba-Biomembranes. 2015;1848(2):496-501. doi: 10.1016/j.bbamem.2014.10.018. PubMed PMID: WOS:000348687500014.